PRAMANA — journal of physics

Vol. 83, No. 6
December 2014
pp. 851–884

Charged particle-induced nuclear fission reactions – Progress and prospects

S KAILAS[1,2,*] and K MAHATA[1]

[1]Nuclear Physics Division, Bhabha Atomic Research Centre, Mumbai 400 085, India
[2]University of Mumbai-Department of Atomic Energy Centre for Excellence in Basic Sciences, Mumbai 400 098, India
*Corresponding author. E-mail: kailas@barc.gov.in

MS received 17 April 2014; revised 13 June 2014; accepted 15 July 2014
DOI: 10.1007/s12043-014-0871-x; ***e*Publication:** 15 November 2014

Abstract. The nuclear fission phenomenon continues to be an enigma, even after nearly 75 years of its discovery. Considerable progress has been made towards understanding the fission process. Both light projectiles and heavy ions have been employed to investigate nuclear fission. An extensive database of the properties of fissionable nuclei has been generated. The theoretical developments to describe the fission phenomenon have kept pace with the progress in the corresponding experimental measurements. As the fission process initiated by the neutrons has been well documented, the present article will be restricted to charged particle-induced fission reactions. The progress made in recent years and the prospects in the area of nuclear fission research will be the focus of this review.

Keywords. Nuclear fission; charged particle-induced fission; heavy ions; fission angular distributions; mass distributions; fission barrier; moment of inertia; shell effect in fission.

PACS Nos 25.70.Jj; 25.85.Ge

1. Introduction

The importance of the technology which has come out of the basic research in nuclear fission need not be overemphasized – the nuclear fission reaction is indeed the heart of any nuclear reactor and the nuclear energy is an inevitable option in the energy mix for many countries in the world. The nuclear fission phenomenon continues to be exciting and interesting from the basic research point of view. The classic paper of Bohr and Wheeler [1] published within a short period of the announcement of the nuclear fission process, still remains the most referred work and has been considered one of the best in terms of our understanding of this phenomenon. The nuclear fission is challenging and complex as it involves large-scale collective motion and drastic rearrangement of nucleons and at the same time exhibiting single-particle aspects in terms of shell effect at large deformation. The fission excitation function, the fission probability, the fission fragment

angular distributions, the mass and kinetic energy distributions, particles emitted prior to and after fission – all these quantities have been measured and considerable progress has been made to understand these features of nuclear fission [2–19]. In the early years, light projectiles like neutrons, protons, deuterons, helions and alphas were employed in these investigations. With the availability of heavier beams, the measurements have been extended to a range of projectiles from lithium to uranium and the fissionable nuclei range in mass numbers from 180 to nearly 260. This has resulted in the detailed investigation of fission process for nuclei at moderately high excitation energies with large angular momentum values. Further, these studies have provided valuable insights into the fission of a large mass number nuclei at deformation values significantly higher compared to ground-state values and the role of nuclear structure at these extreme conditions. It turns out that both statistical and dynamical aspects have to be incorporated in models used to describe the fission process. Dissipation is another aspect that needs to be considered in understanding the fission phenomenon. A comprehensive understanding of the nuclear fission involving heavy nuclei at high excitation energy and spin values as well as the formation and decay of these heavy systems is crucial in the ongoing efforts towards formation of the superheavy nuclei.

In this review, we shall summarize the progress made in our understanding of the charged particle-induced fission reactions and point out the directions in which this research is evolving. In §2, the various nuclear fission observables which are measured experimentally are listed. The related developments in the theoretical formalisms are covered in §3. The three key attributes, viz. dynamics, structure and dissipation which drive fission process are discussed in §4. The emerging areas for nuclear fission research are covered in §5. In §6, the general conclusions are summarized.

2. Nuclear fission observables

The nuclear fission phenomenon has been experimentally investigated through a series of measurements, starting with the famous and pioneering experiments of Hahn and Strassmann [20]. These include the fission fragment angular distributions, the fission excitation functions, the fission fragment mass (kinetic energy) distributions, the folding angle and mass–angle correlation measurements. In general, the fission angular distributions are measured by positioning a number of detectors – thin silicon, gas–silicon hybrid, MWPC etc. and measurements are carried out over the angular range from 90° to 175°. One could also measure from an angle close to 0° up to 90°. But measuring fission data at small angles will be challenging as in this region, the data will be dominated by the elastics. In figure 1a, a typical angular distribution measured for the system F + Os is shown [21]. From the angular distribution data, the total angle integrated fission cross-sections can be determined. The fission excitation function is measured over a range of energies from near the Coulomb barrier to well above the Coulomb barrier. The fission yield is influenced by the Coulomb barrier and also by the fission barrier (B_f). In figure 1b, we have plotted the fission excitation function (cross-section vs. excitation energy of the compound nucleus) for the system ^{19}F + ^{188}Os.

It may be mentioned, that a compound nucleus formed at high excitation energy decays by several channels which are energetically favourable. In the case of heavy fissionable

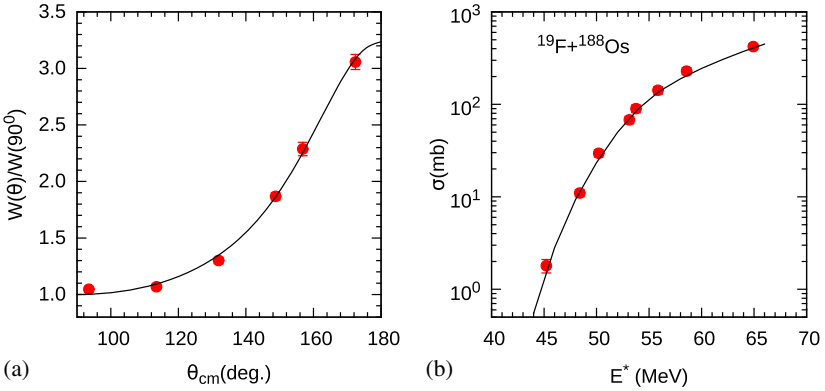

Figure 1. (**a**) Fission fragment angular distribution and (**b**) fission excitation function.

nuclei ($A = 200$–260), the dominant channels are the fission decay and the neutron emission. To have a complete picture of the fissioning process, it is necessary to measure the decay of the compound nucleus through the neutron emission channel. After neutron emission (one or more), from the compound nucleus, heavy residual nuclei are formed. These are called the evaporation residues (ER) and their cross-sections have to be measured along with the fission channel. Adding the fission and the ER cross-sections, one can get the fusion (or compound nucleus formation) cross-section. From a statistical model analysis of these data, the fission barrier can be determined for the fissioning compound nucleus. From the angular distribution data, one can deduce the effective moment of inertia of the fissioning nucleus at the saddle point of deformation. Theses aspects will be discussed in later sections.

Often the fission data may have contributions from complete fusion (CF) (amalgamation of the projectile and the target) and incomplete fusion (ICF) (amalgamation of part of the projectile with the target). It becomes necessary to separate the fission arising from CF (CFF) and that coming from incomplete fusion process (ICFF). This is experimentally accomplished by the fission fragment folding angle technique. Here a detector is positioned at a convenient angle on one side of the target and on the other side of the target another detector is positioned so that both the complementary fragments can be detected in coincidence. Keeping one of the detectors fixed and moving the other over a range of optimized angles, the folding angle distribution can be measured (figure 2 adopted from ref. [22]). In the case of a fissioning nucleus, decaying at rest, the two binary fragments will go in opposite directions, 180° apart. When momentum is given to the decaying compound nucleus (in the real experiment, the compound nucleus formed by the fusion of the projectile and the target is moving with a velocity essentially in the forward direction), the angle between the two fragments will start becoming less than 180°. With increasing momentum given to the compound nucleus, the angle between the complementary fragments will decrease. In figure 2, the peak near 150° is associated with CFF (full momentum transfer from the projectile to the target followed by fission) and the peak near 180° is ascribed to ICFF (partial momentum transfer followed by fission). It should be mentioned that ICFF peak can also come to the left of the CFF peak at smaller angles, depending on the grazing angle. By performing a folding angle distribution

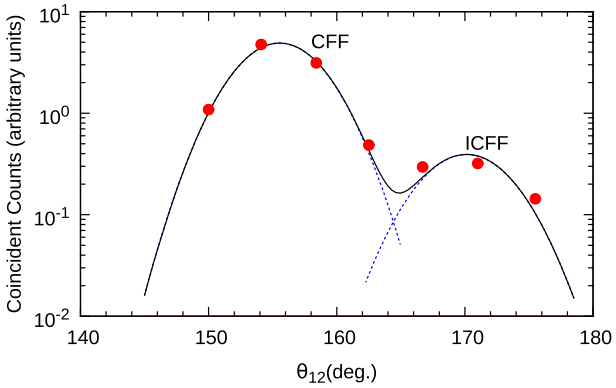

Figure 2. Fission fragment folding distribution.

measurement, it is possible to separate the CFF and the ICFF components as shown in figure 2.

Another quantity which is very important and rather unique to fission is the mass distribution (also kinetic energy distribution). Right from the beginning it was realized that while the binary fragments result from each fission event, there is also a mass (charge) distribution associated with the fragments. It is also true for the kinetic energy distribution of the fragments. Of course the mass and charge conservation of the resulting fragments will be consistent with the mass and charge of the fissioning nucleus. In figure 3, we have shown the fission fragment mass distribution for neutron-induced fission of ^{239}Pu (compound nucleus ^{240}Pu) at two bombarding energies, 0.5 and 14 MeV. It may be noted that the distribution becomes more symmetric at 14 MeV, from an asymmetric distribution observed at lower energy. Mass distribution can be measured by measuring the velocities (related to the time-of-flight of the fragments from the target to the detector) and the energies of the complementary fragments. It can be seen that as a function of the bombarding

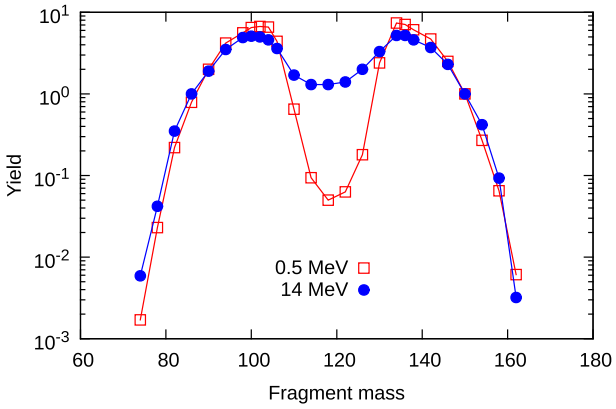

Figure 3. Fission fragment mass distribution (data taken from ref. [23]).

energy (as a function of the excitation energy of the fissioning compound nucleus), the mass distribution changes from asymmetric to symmetric mass distribution.

The mass distribution has been one of the puzzling features of fission phenomenon right from inception and even after 75 years of research, the mechanism of mass division is not fully understood. Later, mass separators for fission fragments (like LOHENGRIN) were used for the detection of fragments with better mass resolution [24]. In recent years, high-energy radioactive ion beams, produced from the fragmentation of 1 A GeV ^{238}U have been mass separated and made to undergo electromagnetic excitation interacting with a Pb target. This way it has been possible to study the fission of many nuclei away from the line of stability at low excitation energies, around 11 MeV [25]. The beta delayed fission is another tool to study fission of nuclei at low excitation energies [19]. This technique has been employed for measuring mass distribution of ^{180}Hg. More recently, high-energy heavy beams like ^{238}U have been made to impinge on a lighter target like ^{12}C to measure fission fragments. In using this inverse kinematics technique, it has been possible to obtain fragments with high energies, thereby facilitating the detection of the same with good mass and charge resolution with a mass spectrometer. Using this technique, it has been possible to obtain the fission fragments arising from fission, following the fusion of the projectile (^{238}U) and the target (^{12}C) – compound nucleus ^{250}Cf as well as fission following the transfer of a few nucleons (two protons) from the target to the projectile (resultant composite system ^{240}Pu). The fragments spanning a large range of Z (30–64) and A (80–160) have been measured by this technique [26].

As mentioned earlier, the study of mass distribution of fission fragments has been attracting the attention of the investigators right from the beginning of nuclear fission research. This field of research has been recently reviewed by Schmidt [27] and Andreyev [28]. Thermal neutron-induced fission of ^{235}U leads to asymmetric mass division with the most probable masses to be m_{H} (heavy fragment) $\approx$140 and m_{L} (light fragment) $\approx$96. However, the maximum kinetic energy is observed for the mass split with m_{H} varying from 130 to 135 and the corresponding m_{L} varying from 106 to 101. The asymmetric mass division usually found in the fission of actinides is taken as evidence for the presence of shell correction in the fissioning nucleus. It is fascinating (figure 4) to observe that while the heavier actinide nuclei with large N/Z predominantly undergo asymmetric

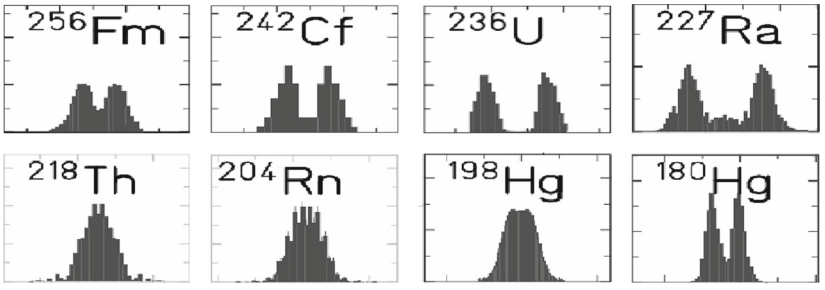

Figure 4. The mass distribution systematics plotted for nuclei with A varying from 180 to 256 (data taken from Schmidt [27] and Andreyev [28]). It is interesting to note the change from mass asymmetric division to symmetric division as A and N/Z values are decreased. Further decrease brings back the mass asymmetry in fission.

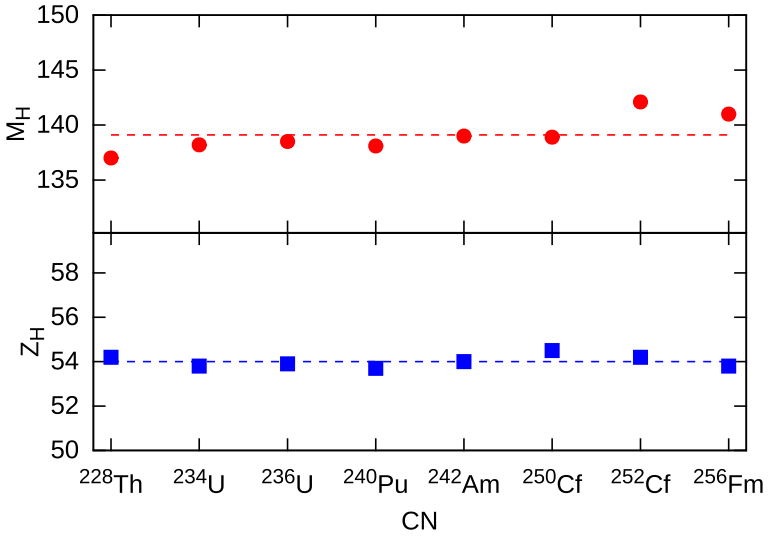

Figure 5. The peak values of mass distribution – the heavy fragment charge (Z_H) and heavy fragment mass (M_H) are plotted as a function of A of the fissioning nuclei (data taken from refs [25,27,29]).

mass division, the lighter nuclei, Ir–Th with N/Z around 1.45, exhibit dominantly symmetric mass division. When we go to lower A and N/Z values (1.25), mass distribution pattern changes to one of asymmetric mass division. It is fair to state that only a qualitative understanding of the various features of mass division are understood in terms of scission point or dynamical model.

It is intriguing (figure 5) to find for a series of nuclei A 220–260, the average charge number of the heavy fragment is around $Z = 54$ [25,27,29], the charge of the number of

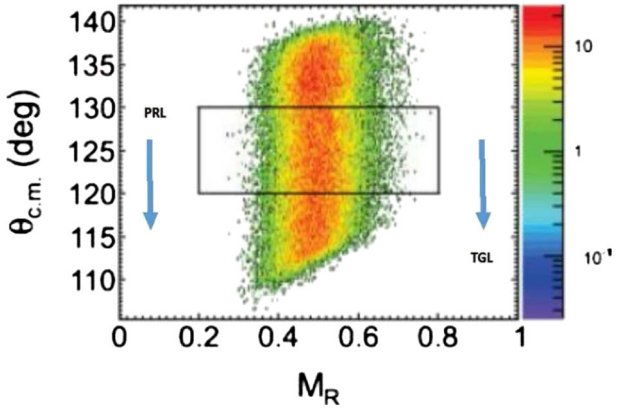

Figure 6. Correlation between mass of the fission fragment and angle of detection. $M_R = m_2/(m_1 + m_2)$ where ms are the masses of the two fragments. PRL = projectile-like fragments, TGL = target-like fragments.

light fragment varies with the mass/charge of the compound nucleus. The heavy fragment mass is also around $A = 139$. For neutron-deficient actinides, the heavy fragment mass is lower than 139 by a few mass numbers. We have plotted in the figure a few values of the average Z and A values for the heavy fragments arising from the fission of actinides lying in the above mass region. Further, the nucleus with $Z = 54$ and $A = 139$ will have $N = 85$. We know that both $Z = 54$ and $N = 85$ do not form part of the magic numbers. It is not fully understood as to why these N and Z values are preferred.

In figure 6, we have shown a typical fragment mass–angle correlation (adopted from ref. [30]). The symmetric mass division is clearly seen corresponding to MR = 0.5. The PRL and TGL arise from non-compound process. The neutrons and charged particles are also detected in coincidence with the fission events, in order to have a handle on the fission dynamics as the particles are emitted from the composite system through the formation, capture and the equilibrium stages of fusion–fission process. These particle multiplicity measurements are also essential to deduce information regarding the dissipation aspects of fission. Both light (like neutrons, protons, alphas) and heavy ions have been employed in these investigations. In the former case, the excitation energies and the angular momenta involved are relatively small when compared to that obtained by using the heavy ions. In the case of light ions, the pre-equilibrium emission process competes with the compound nuclear process at energies E/A about 8 MeV or so. While employing the heavy ions, the non-compound fission events like fast fission, quasifission, pre-equilibrium fission and transfer fission interfere with the full momentum transferred compound nuclear fission detection. It is necessary to separate these non-compound events to obtain data for pure compound nuclear fission.

3. Theoretical formalisms

Within a short time after the announcement of nuclear fission, Bohr and Wheeler [1] came with a masterly article on the mechanism of nuclear fission. They argued that nuclear fission phenomenon is due to the competition between the disruptive Coulomb interaction and the attractive surface tension. Amongst other things, using the charged liquid drop model, they estimated the fission barrier height for several nuclei, kinetic energy and mass division in fission. They also pointed out that it was the less abundant isotope ^{235}U which underwent fission with thermal neutrons and not the heavier and more abundant ^{238}U. They could describe well the decay of excited compound nuclei through the fission and the neutron channels. In general, a theory of nuclear fission should be able to address the following features observed experimentally:

(1) Stability limit for fission.
(2) Spontaneous fission and the barrier height.
(3) Fission decay of the compound nucleus as a function of the excitation energy.
(4) Nuclear dissipation, fission delay time and the pre-fission emission of particles at higher excitation energy of the fissioning nucleus.
(5) Symmetric and asymmetric mass division of the fissioning nucleus.

It is indeed a formidable task to have one model which can account for all these properties.

The charged liquid drop model is fairly successful in explaining the deformation of the fissioning nucleus from the equilibrium shape to the scission stage through the saddle point. The observation of fission isomers [31], the sub-barrier resonances and the asymmetric mass distribution clearly indicated the need for the inclusion of single-particle effects in the above model. In fact, Mayer who proposed the shell model of the nucleus observed [32] that the magic numbers 50, 82 associated with neutrons/protons could be responsible for the asymmetric mass division with heavy fragments close to these numbers. Shell effect as a function of deformation had to be included and Strutinsky [33] came out with a prescription about how this could be accomplished. Finding the shell effect at large deformation is a crucial step in our understanding of the nuclear fission phenomenon. As a result of the addition of deformation-dependent shell correction to the liquid drop potential energy as a function of deformation, the resultant potential energy becomes a double-humped barrier [3] (this is shown in figure 7b). While there are two barriers (outer and inner) for most of the actinides, the barrier becomes single valued for the lighter pre-actinides (A less than 210 or so) in general. The concept of double-humped barrier provided explanation for the existence of fission isomers and sub-barrier resonances. The shell effect is also important in understanding the mass division. The most important application of shell effect at large deformation is the prediction of stability of nuclei far away from the line of stability, the superheavy region. The non-zero barrier predicted for superheavy nuclei needs to be confirmed through the experimental detection of the superheavy nuclei. It has been recognized that to understand the broad features of fission, both the macroscopic (liquid drop) and the microscopic (shell model) features have to be considered. Both statistical and dynamical aspects are essential to describe the fission observables. In addition, the dissipation or viscosity is also an important feature which needs to be considered for understanding the fission phenomena. Fissility parameter is defined as $x = Z^2/A[50.8831 - k((N-Z)/A)^2]^{-1}$ ($k = 1.7826$ and it could be varied) and $x = 1$ is the limit of stability against fission. A, Z and N are related to the fissioning nucleus. The mildly deformed ground state (A), the saddle point (B) and the scission point (C) are the three decision-making points of the deforming fissioning nucleus (figure 7) [11]. It is now accepted that the fission process takes a fairly long time, starting with the capture of the projectile by the target through the formation of the compound nucleus and finally the fission stage. It has been estimated that the fission process takes place over a time, about 30×10^{-21} s [10]. During the transit over the saddle, there is also a possibility that a part of the flux can diffuse to the left side, thus reducing the fission probability. This was recognized by Kramers way back in 1940 [34]. Particles and gammas can be emitted all through these decision-making stages if energetically allowed. More details about the fission dynamics and dissipation can be found in refs [7,10]. Due to the viscous nature of the nuclear fluid, the time taken to diffuse through the saddle and scission stages is lengthened. In essence, the fission probability gets reduced. This aspect is further discussed later in the section.

The statistical model is successful in describing the decay of the excited compound nucleus [2,7,35]. For the fissionable heavy nuclei under discussion, the dominant decay channels are fission and neutron emission. The fission width Γ_f is defined as

$$2\pi\Gamma_f/D(E_x) = \int_0^{E_x - B_f} \rho(E_x - B_f - K)\mathrm{d}K, \tag{1}$$

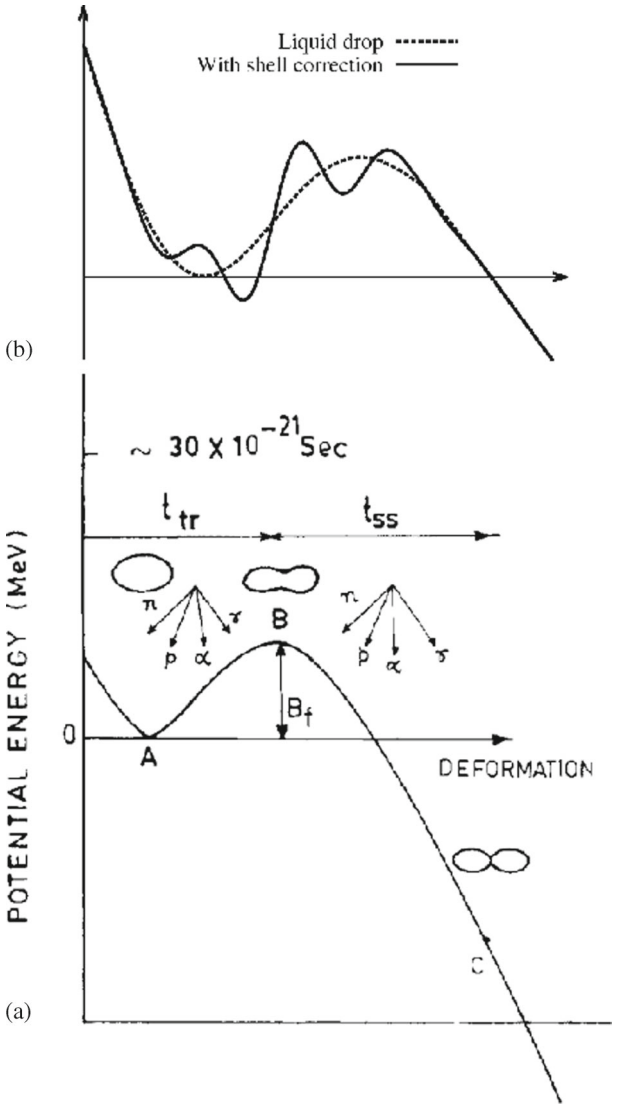

Figure 7. (**a**) Schematic of the fissioning nucleus showing the decision making points. A represents the ground state, B the saddle point and C the scission point of the deforming nucleus. t_{tr} and t_{ss} are the fission times upto the saddle stage and the scission point respectively. (**b**) The change to the liquid drop barrier when deformation-dependent shell effects are included. For actinides in general, the addition of shell contribution to the liquid drop potential energy, leads to a double-humped barrier as shown in the figure. The dotted line is the liquid drop potential and the solid line is the potential energy when deformation-dependent shell contribution is added.

where D is the level spacing in the compound nucleus (fissioning nucleus), K is the kinetic energy in fission degree of freedom and ρ is the level density at the saddle point. The neutron width Γ_n is defined as

$$2\pi\Gamma_n/D(E_x) = 4mR^2/\hbar^2 \int_0^{E_x - B_n} \epsilon\rho(E_x - B_n - \epsilon)d\epsilon, \quad (2)$$

where m is the nucleon mass, R is the size of the fissioning nucleus, ρ is the level density at the residual nucleus after neutron emission and ϵ is the energy carried by the neutron. The level density $\rho(x)$ can be written as $\exp(2\sqrt{ax})$. Here a is the level density parameter defined as $a = A/8.5$ (typical value). A is the mass number. More details can be found in refs [2,35]. Using this relation, the ratio of fission and neutron decay probabilities is given approximately as the ratio of the respective level densities at the saddle point and the residual nucleus after neutron emission (see figure 8).

$$\Gamma_f/\Gamma_n \approx \rho(E_x - B_f)/\rho(E_x - B_n)$$
$$\approx \exp(2[\sqrt{a_f(E_x - B_f)} - \sqrt{a_n(E_x - B_n)}]). \quad (3)$$

The a's are the level density parameters at the saddle point and for the residual nucleus after neutron emission. In writing this simple expression for the decay widths we have not considered the corrections for the rotational energy.

Basically, the decay widths are dominated by the phase-space available, viz. the level densities at the saddle and the residual nucleus. Depending upon the B_f and B_n values, the

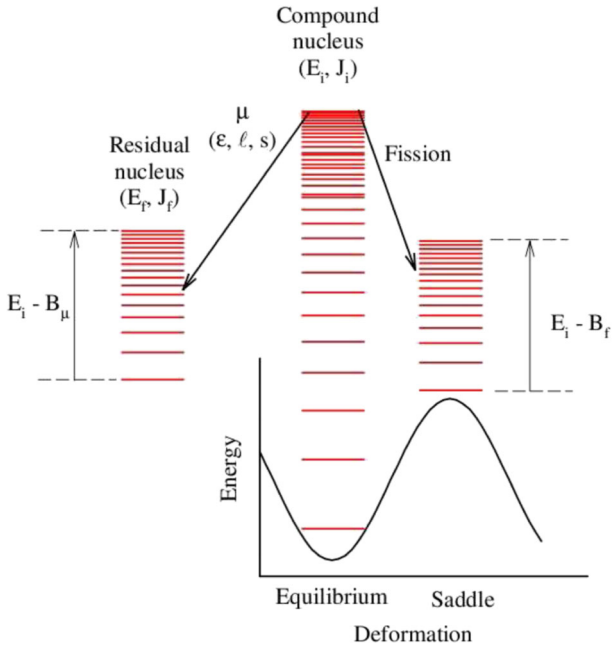

Figure 8. The excitation energy (E_i – initial value, same as E_x) of the compound nucleus, the levels in the compound nucleus (CN), the residual nucleus (after neutron (particle μ) emission) (RN) and the saddle point are shown in the figure.

ratio of fission to neutron decay probability changes with excitation energy. More details of the statistical model treatment of the compound nucleus decay can be found in refs [2,35]. The fission excitation function and the angular distribution data can be understood in terms of the above statistical model. To predict the latter quantity, a knowledge of the saddle-point deformation and the related moment of inertia will be required.

Usually, the time taken from the equilibrium to saddle and beyond is taken to be small when compared to the neutron emission lifetime for actinide nuclei at lower excitation energies. In essence, the fission decay probability dominates over the neutron decay if the fission channel is energetically allowed. This is generally true for E_x up to around 50 MeV. Above this energy, it is observed that a substantially large number of pre-fission neutrons are emitted (significantly larger than the statistical model estimates). This feature could be understood only by slowing down the fission decay (reduction of the fission decay probability) in comparison to neutron emission over some time period. It turns out that at these high excitation energies, the neutron emission lifetime begins to compete with the lifetime associated with the collective degree of freedom related to fission (dynamical delay time of fission). Due to the viscous nature of the nuclear fluid, the fission probability becomes time-dependent. This being the case during the fission delay time (the transient time taken for the fission probability to build up to the stationary value – time taken from the equilibrium deformation to the saddle point), additional neutrons are emitted. Thus, by slowing down the fission decay probability over a time period (transient time), emission of additional neutrons is facilitated. Taking into account the viscous nature of the nuclear fluid, the relaxation time from the equilibrium deformation to the saddle point and beyond can be estimated. The transient time from equilibrium deformation to the saddle point is given as $t_f = [\gamma/\omega] \ln(10B_f/T)$ [6,7,9,10], where ω is the barrier assault frequency and T is the nuclear temperature. For $B_f = 10$ MeV and $T = 2$ MeV, t_f is estimated to be 3.9×10^{-20} s if $\gamma = 10$ [9]. The fission width becomes time-dependent and is given as

$$\Gamma_F(t) = \Gamma_K[1 - \exp(-t/t_f)] \tag{4}$$

and

$$\Gamma_K = \Gamma_f(\sqrt{1+\gamma^2} - \gamma). \tag{5}$$

Here Γ_K is the Kramers width [34] which takes into account the possible diffusion of flux from saddle towards equilibrium deformation and γ is the friction coefficient. If $\gamma = 1$, then Γ_K becomes $0.4 \times \Gamma_f$. By following the procedure outlined above, it has been possible to bring in the concept of nuclear dissipation (nuclear viscosity) responsible for the delay in the fission process, accompanied by enhanced emission of neutrons. γ is also defined as $\gamma = \beta/(2\omega)$ [7,10] as the ratio of reduced frictional (dissipation) coefficient (β) and the assault frequency. Thus, we see that the fission width gets reduced due to two factors: one due to Kramers diffusion and the other due to dissipative or friction (viscosity) effects. In fact, using the pre-fission neutron emission time as a clock, it has been possible to measure the time taken by the fissioning system to evolve from the equilibrium shape to scission point. While the saddle to scission time is large in the case of actinides, it is relatively short in the case of nuclei lighter than actinides and with mass numbers close to 200. Typical value of nuclear viscosity estimated is 1–3$\times$ 10^{12} cP and it can be compared with the values of 1 cP and 10000 cP respectively for

water and honey [36]. More details of the role of dissipation in fission can be found elsewhere [6,9,10,37]. As mentioned earlier, the fission delay time due to the viscous nature of the nuclear fluid is estimated to be of the order of 10^{-21} to 10^{-20} s. Thus, the emission of a larger number of pre-fission neutrons in comparison to the statistical model can be understood by invoking the nuclear viscosity and dynamical delay time of fission.

The fission angular distributions are generally described in terms of the transition state model. According to the saddle point statistical model (saddle point is the main decision-making point on the way to fission), the fission fragments are emitted along the symmetry axis. The total angular momentum of the fissioning nucleus is taken as J and its projection on the symmetry axis is K. In this model, the K value (K distribution) is preserved between the saddle and the scission points. The transition state nuclei are assumed to be axially symmetric. The angular distribution of the fission fragments for each state (specified by J and K) is given by the symmetric top wave function $\mathrm{D}^{J}_{MK}(\theta)$. The angle between the symmetry axis and the beam axis is taken as θ. The target and projectile spins are taken to be zero for the present discussion. In that case $J = \ell$, the orbital angular momentum. The distribution of K is given as

$$\rho(K) = \exp(-K^2/(2K_0^2))/\sum \exp(-K^2/(2K_0^2)). \tag{6}$$

Here $K_0^2 = I_{\mathrm{eff}}T/\hbar^2$ with $1/I_{\mathrm{eff}} = 1/I_{\mathrm{pa}} - 1/I_{\mathrm{pe}}$, where I_{eff} is the effective moment of inertia at the saddle point, I_{pa} and I_{pe} are the moments of inertia parallel to and perpendicular to the symmetry axis, T is the temperature at the saddle point. The expression for fission fragment angular distribution [2,6,11,45] is then given as

$$W(\theta) = (\pi/k^2)\sum(2\ell+1)T_\ell \sum(2\ell+1)D^{\ell}_{0K}(\theta)^2\rho(K). \tag{7}$$

The fission fragment anisotropy is given as $A = W(0^\circ)$ or $W(180^\circ)\,/\,W(90^\circ)$ and the above complex expression can be simplified as

$$A \approx 1 + \frac{\langle \ell^2 \rangle}{4K_0^2} = 1 + \frac{\langle \ell^2 \rangle}{4I_{\mathrm{eff}}T}. \tag{8}$$

(I_{eff} is the effective moment of inertia and T is the temperature at the saddle point. $\langle \ell^2 \rangle$ is the second moment of the angular momentum distribution of the compound nucleus related to fission part of the compound nuclear decay). The effective excitation energy at the saddle point is given as $E_x(\mathrm{saddle}) = E_x(\mathrm{of\ the\ compound\ nucleus}) - B_{\mathrm{f}} -$ rotational energy $-E_{\mathrm{n}}$ (energy removed by neutrons emitted from the fissioning nucleus before reaching the saddle point – the pre-fission neutrons). The temperature at the saddle is given as $T = \sqrt{E_x(\mathrm{saddle})/a_{\mathrm{f}}}$. Here a_{f} is the level density parameter at the saddle point. More details of angular distribution can be found in ref. [2]. From a statistical model analysis of the angular distribution data, it is possible to get values of the effective moment of inertia at the saddle and hence the deformation of the fissioning nucleus at this decision-making point.

Another unique feature of nuclear fission is the mass distribution exhibited by the fissioning nucleus. Related to this is the kinetic energy carried by fragments. The kinetic energy systematics has been provided by Viola *et al* [38]. The kinetic energy is empirically given as $\mathrm{KE} = 0.1166Z^2/A^{1/3} + 9$ MeV. The scission point is generally considered approximately as the decision-making point in the potential energy surface where the

compound nucleus splits into two fragments, releasing energy. Interestingly, the KE measured in fission is almost independent of the bombarding energy of the projectile.

The questions that will be interesting to answer are: at what stage the fissioning nucleus decides a preferred mass division? What are the roles of potential energy surface and shell effect in this decision? What are the factors which influence the width of the mass distribution? Any theory proposed should also address all the experimental observables mentioned above. We shall now give a jist of the various theories proposed. Some of the earlier successful models proposed were based on the scission point as the key to mass division. These models are discussed by Wilkins *et al* [39] and Brosa *et al* [40]. The more sophisticated models proposed in recent times are due to Warda *et al* [41], Ichikawa *et al* [42] and Aritomo and Chiba [43]. Aritomo and Chiba have carried out a fully dynamical model, from equilibrium shape to scission point through the saddle point. The pre-scission emission of particles is also taken into account in this prescription. This is a dynamical model involving Langevin equation based on the fluctuation dissipation theorem. They also considered the shell effect in their model. Though dynamical models have been used at higher excitation energies, Aritomo and Chiba have extended this calculation to lower excitation energies by adopting advanced computational techniques. They have made calculations of mass distributions for a number of systems ^{234,236,238}U and ^{240}Pu. They have obtained satisfactory agreement with the mass distribution data. While they predicted the position of the heavy fragments peak, their calculations somewhat overpredicted the peak position of the light fragments. The widths calculated are consistent with the measured data. According to them, while the peak positions in the mass distributions are decided at the saddle point in the potential energy landscape which includes the shell correction energy, the width of the mass distributions are influenced strongly by the shape fluctuation near the scission point. A random walk method of Randrup and Moller [44] is also successful in describing the mass distribution data of actinides. Interestingly, both $Z = 54$ and $N = 85$ do not correspond to any known magic number. These values are close to magic numbers $Z = 50$ and $N = 82$ (spherical), 88 (deformed). Some models have been proposed to describe the peak in the mass distribution around $A = 140$ as arising due to $N = 82$ and $N = 88$ magic numbers.

Recently, it was observed [45] that the fission of a nucleus like ^{180}Hg does not lead to symmetric mass division of fragments, ^{90}Zr ($Z = 40$, $N = 50$) expected from the shell correction in the fragment as well as liquid drop model considerations but to two unequal mass fragments with masses around Kr-80 and Ru-100. This finding has generated a lot of interest about the role of shell closure in influencing the mass distribution. The observation of asymmetric mass division in the neutron deficient ^{180}Hg is in contrast with the relatively symmetric mass division seen for the heavier Hg isotope, ^{198}Hg. Warda *et al* [41] proposed the energy density functional approach to describe the mass division in the case of Hg isotopes. They suggested that the presence of shell effect in the pre-scission region is influencing the mass division. They could predict a gradual transition from the more asymmetric mass distribution in the case of lighter Hg isotopes to a more symmetric mass split for the heavier Hg isotopes. Ichikawa *et al* [42] have computed potential energy surface using the macroscopic–microscopic approach as functions of five shape coordinates for more than five million shapes. They have calculated minima, saddle points, valleys and ridges. According to them, in the case of ^{180}Hg, the fission barrier height and the ridge values are such that the saddle point was getting shielded from a deep symmetric

valley. Hence, the lighter Hg isotopes prefer to undergo asymmetric mass division. However, in the case of heavier Hg isotopes, the ridge becomes less important facilitating symmetric mass division. They did not find any significant role for the shell closure in the fragments in describing the Hg isotopes. However, they found that the shell closure has a role to play in the case of fission of actinides. While the scission point model of Wilkins *et al* assumed that the statistical equilibrium was reached at the scission point, the improved model due to Andreev *et al* [46] has relaxed this requirement. Using this model, Andreev *et al* [46] have been able to describe the mass distribution data of the Hg isotopes.

4. Dynamics, structure and dissipation influencing fusion–fission reactions

In the previous sections we had seen the experimental observables and the theoretical models developed to describe the data. In dealing with the fusion–fission reactions, broadly there are three aspects which have to be considered as they influence the fusion–fission process: (1) Dynamics – Amongst other things, the reaction dynamics depends on the bombarding energy, the fusion barrier, the entrance channel mass (charge) asymmetry $((A_T - A_P)/(A_T + A_P))$ and the fissility. (2) Structure – The nuclear structure of the interacting nuclei and the intermediate composite system, the structure at the equilibrium deformation (ground state), saddle point and the scission point of the fissioning nucleus. The fission barrier and the level density are the two most important quantities in any fission-related theoretical model. Both depend strongly on nuclear structure. (3) Dissipation – The nuclear viscosity is the third factor which influences the fission. In fact the dissipation or nuclear viscosity of the fissioning nucleus was inferred right in the beginning of fission research by Kramers. The viscous nature of the nuclear fluid is the one which decides the time-scale of fission – the time taken by the fissioning nucleus from the equilibrium deformation to the saddle and beyond up to the scission point is mainly decided by the dissipation or the viscosity of the deforming nucleus.

One may broadly categorize the different stages of evolution of the heavy-ion induced fusion–fission reactions as follows: In general there are three stages of evolution: the capture (cap) of the projectile by the target to form a composite system; the evolution of this intermediate system towards a fully equilibrated compound nucleus (cn); the decay of the compound nucleus into fission (cnfiss) and evaporation residue (er) channels. It has been observed that in a few situations non-compound fission (ncnfiss) like events can also arise as the composite system evolves towards the compound nucleus. In essence, the fission measurements will contain both cn and ncn fission contributions.

$$\sigma_{\text{cap}} = \sigma_{\text{fus}} + \sigma_{\text{ncnfiss}} \tag{9}$$

and

$$\sigma_{\text{fus}} = \sigma_{\text{er}} + \sigma_{\text{cnfiss}}. \tag{10}$$

Hence,

$$\sigma_{\text{fiss}} = \sigma_{\text{ncnfiss}} + \sigma_{\text{cnfiss}}. \tag{11}$$

Experimentally, the challenge is to disentangle between these components of fission before interpretation of the data can be attempted. The nuclear structure and the

dynamics influence all the three stages as discussed above. The role of nuclear structure and dynamics in influencing fusion–fission reactions has been reviewed some years ago by Kailas [11]. The heavy-ion fusion process has been discussed extensively in the literature (see ref. [47] for the latest review). The evolution of the intermediate composite system towards a fully equilibrated compound nucleus (along with the emission of non-compound fission events during this stage) and the subsequent decay of the excited compound nucleus into evaporation and fission components have been discussed extensively (ref. [13] and the related references contained here). In addition to nuclear structure and dynamics, it is also necessary to take into account the viscous nature of the nuclear fluid in any model developed to describe the fission phenomena and understand the measured observables. In the following sections, we shall discuss specifically the experimental measurements and analysis which corroborate the strong influence of dynamics, structure and dissipation on nuclear fission.

4.1 *Reaction dynamics – Role of entrance channel*

The nuclear fission dynamics has been discussed extensively in [5–7,13,48,49]. There are three types of non-compound nuclear fission processes [11]: If the fission barrier is close to zero, the phenomenon of fast-fission (FF) [50,51] will occur. If the saddle point is more compact when compared to the entrance channel contact configuration then quasifission (QF) [48,52–54] will take place. But even when the system is formed with the entrance channel more compact than the saddle point, if the system is not equilibrated in K degree of freedom (K is the projection of angular momentum of the compound nucleus on the symmetry axis of the fissioning nucleus) or shape degree of freedom then the pre-equilibrium fission (PEQF) [55,56] will take place. According to the PEQF model, the entrance channel mass asymmetry is expected to play a strong role in influencing the dynamics. For systems having entrance channel mass asymmetry $\alpha(= (A_T - A_P)/(A_T + A_P))$ greater than a critical value (α_{BG}), the driving force after capture of the projectile by the target will be to make the system more asymmetric. In this case, the heavier target will absorb the lighter projectile to form the compound nucleus. However, if the entrance channel α is less than α_{BG}, after capture the driving force will be to make the system more symmetric, i.e. to say that projectile will grow in size at the expense of the target. During this process the system can re-separate as two fragments as in fission. The system in this case has memory of the entrance channel (narrow K distribution) and hence the fission anisotropy values for these events are expected to be significantly larger than that for the compound nuclear fission values. Thus, the experimental signature for the occurrence of PEQF will be the observation of the entrance channel dependence of fission anisotropy values across α_{BG}. In other words, one expects 'normal' anisotropy values consistent with the saddle point statistical model for systems with entrance channel α greater than α_{BG}, and 'anomalous' values significantly larger than the saddle point predictions for systems with α less than α_{BG}.

In a series of experiments, Ramamurthy *et al* [56] provided the experimental signature for the presence of PEQF in addition to compound nucleus fission. This feature has been demonstrated [57] in several systems with ^{232}Th as the target. In figure 9, the fission anisotropy values measured are shown as a function of bombarding energy. It can be seen from the figure that the data are in agreement with the calculations for the

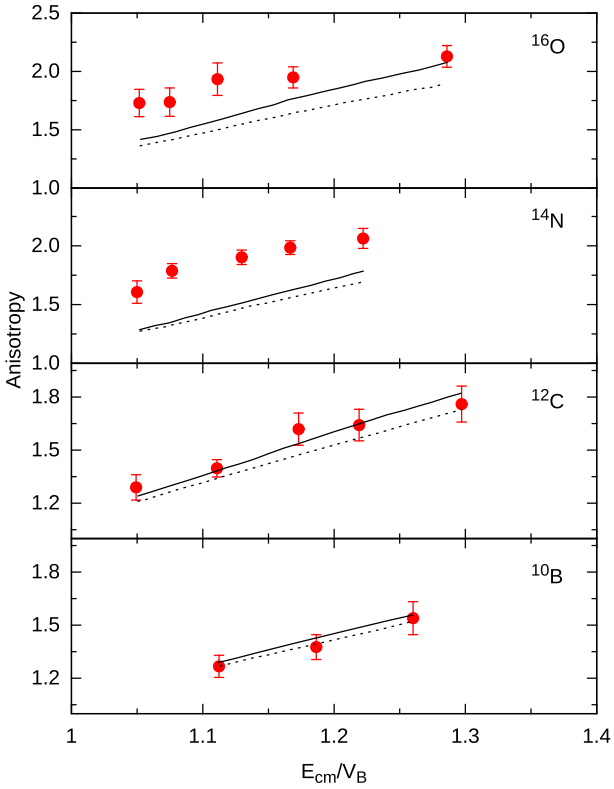

Figure 9. Fission anisotropy values for different projectiles interacting with ^{232}Th target. The α values are 0.917, 0.902, 0.886 and 0.871 respectively for B, C, N and O plus Th systems. The average α_{BG} is 0.893. Saddle-point calculations with and without pre-saddle neutron emission corrections are shown as continuous and dotted lines respectively (ref. [57]).

projectiles ^{10}B and ^{12}C. These systems having the α values more than the α_{BG} values are considered 'normal' as data agree with the saddle point model calculations. In the case of heavier projectiles, ^{14}N and ^{16}O, having α values smaller than α_{BG} values, the data are not consistent with the calculations. These are considered 'anomalous' due to the presence of both compound and pre-equilibrium fission components. Thus, a transition from 'normal' to 'anomalous' values of anisotropies takes place between the two systems employing the projectiles C and N. This observation is consistent with the expectation of the PEQF model. However, in these studies, the compound nuclei populated are not the same. Hence it is important to carry out these studies for different entrant channels populating the same compound nucleus. The presence of PEQF has been conclusively shown in systematic studies for several systems (α values are shown in brackets) – ^{11}B + ^{237}Np (0.911), ^{12}C + ^{236}U (0.903), ^{13}C + ^{235}U (0.895) and ^{16}O + ^{232}Th (0.871) having different entrance channel mass asymmetry values but forming the same compound ^{248}Cf [58]. The transition from 'normal' to 'anomalous' values of anisotropies for systems with mass asymmetries lying on either side of $\alpha_{BG} = 0.897$ is clearly brought out in figure 10.

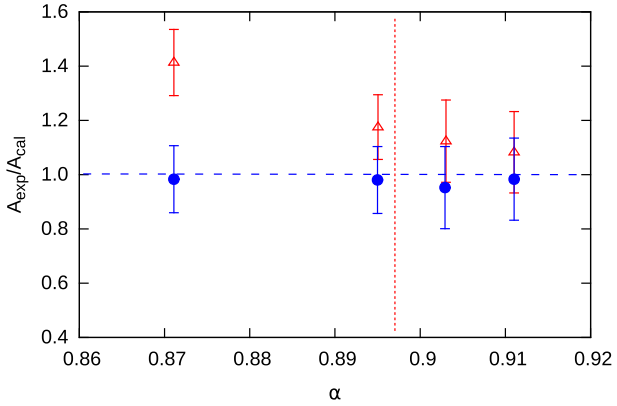

Figure 10. The ratio of experimental and calculated values of anisotropy for different entrance channels: $^{11}B + ^{237}Np$, $^{12}C + ^{236}U$, $^{13}C + ^{235}U$ and $^{16}O + ^{232}Th$ are shown. The open squares are obtained using the standard statistical model and the filled squares are obtained using the PEQF and CNF contributions (calculation details in ref. [59]).

For systems exhibiting PEQF, additional contributions to anisotropies arising due to PEQF have been estimated using the prescription of Thomas *et al* [59]. It should be noted that PEQF will occur only if both entrance channel mass asymmetry and B_f/T (ratio of fission barrier to saddle point temperature) are favourable, viz. α less than α_{BG} and B_f comparable to T. In the above examples, the latter condition was always satisfied. However, if B_f values are significantly larger than T, PEQF fraction will be insignificant even if the entrance channel mass asymmetry values are less than α_{BG}. This fact has been brought out by Tripathi *et al* [60], who studied the systems $^{28}Si + ^{176}Yb$ and $^{16}O + ^{188}Os$ forming the same compound ^{204}Po. Even though the two systems have α values on either side of α_{BG}, both systems exhibit normal values of anisotropies consistent with the saddle-point calculations, implying the absence of PEQF. This is attributed to the relatively large values of B_f when compared to T for these systems. They also did not find evidence for quasifission. Appannababu *et al* [61] have extended these investigations to systems $^{11}B + ^{204}Pb$ and $^{18}O + ^{197}Au$ forming the compound nucleus ^{215}Fr and reached a conclusion similar to that of Tripathi *et al*. From the above discussion, it is implied that when part of the flux from capture to compound nucleus stages is lost due to non-compound fission like QF, then there should be a reduction in contribution of the corresponding evaporation residue.

In several studies of fusion–fission measurements, Hinde *et al* [62] and Sagaidak *et al* [63] have reported the observation of hindrance to evaporation residue (ER) formation (reduction of ER cross-section) in systems which also exhibit QF. They also noted that for a given compound nucleus, the projectile–target system which is more symmetric exhibited quasifission, accompanied by a reduction in ER. While the more symmetric system, $^{30}Si + ^{186}W$, showed a suppression of ER due to the presence of QF, the more asymmetric system $^{12}C + ^{204}Pb$ did not show suppression of ER and exhibited only compound nuclear fission. It may be noted that both these systems lead to the same compound nucleus. While Hinde *et al* found suppression of fusion for the system $^{19}F + ^{197}Au$

(implying the presence of QF), Tripathi *et al* [64] found that the fission fragment angular distribution for this system was normal, consistent with the saddle-point predictions (implying the absence of QF). Similarly, Nishio *et al* [65] who measured evaporation residues for the system $^{16}O + ^{238}U$, found that the data could be well understood through the statistical decay of a compound nucleus. This result is again in contrast to the earlier work of the Canberra group who found the presence of QF in the above system (meaning that there should be a suppression of fusion).

Mitsuoke *et al* [66], Liang *et al* [67] and Satou *et al* [68] have observed enhancement of fusion for reactions initiated by projectiles/targets having neutron or proton magic numbers. Mitsuoke *et al* observed that the evaporation residue cross-section for the system $^{82}Se + ^{138}Ba$ was significantly larger than that measured for $^{82}Se + ^{134}Ba$. This result is attributed to the former system having $N = 82$, a magic number in the target ^{138}Ba. Moller and Sierk [69] have argued that because of the neutron shell closure of one of the interacting nuclei, there is resistance to deformation during the collision. This leads to closer interaction between the projectile and the target, leading to the higher probability of formation of compound nucleus. It follows that the systems having at least one of the interacting species with magic number of neutrons, will have less of QF compared to the system with both the species having neuron numbers away from the magic numbers. Choudhury and Thomas [70] have tried to provide a systematics of the various mechanisms which take place during heavy-ion-induced fusion + fission reactions. The entrance channel and compound nucleus fissility values are defined as:

$$\chi_{\text{eff}} = (Z^2/A)_{\text{eff}}/(Z^2/A)_{\text{crit}}$$

with

$$(Z^2/A)_{\text{eff}} = 4Z_{\text{P}}Z_{\text{T}}/(A_{\text{P}}^{1/3}A_{\text{T}}^{1/3}(A_{\text{P}}^{1/3} + A_{\text{T}}^{1/3}))$$

and

$$\chi_{\text{CN}} = (Z_{\text{CN}}^2/A_{\text{CN}})/(Z^2/A)_{\text{crit}},$$

where $(Z^2/A)_{\text{crit}} = 50.88(1 - 1.783I^2)$ with $I = (A_{\text{CN}} - 2Z_{\text{CN}})/A_{\text{CN}}$ and they have been used to bring out the systematics. They have indicated the regions/systems which are exhibiting compound nuclear fission, pre-equilibrium fission and quasifission. Soheyli and Khalili [71] have also provided a similar systematics with a plot of A_{P} and A_{T} to categorize the region below which we have compound nuclear fission and outside this line it will be non-compound nuclear fission. Zhang *et al* have attempted to separate the two components in a model assuming that the larger ℓs contributed to QF and the smaller ℓs to CN [72]. It is clear that there are various quantities – the target and the projectile mass numbers, the shell closure of the interacting nuclei, the product of their atomic numbers, the bombarding energy, the entrance channel mass asymmetry, the compound nucleus mass and fissility values – which contribute to the presence/absence of the compound/non-compound fission process.

It is generally observed that systems having fissility values larger than 0.723 and/or charge product, $Z_{\text{P}}Z_{\text{T}}$ more than 1600, are expected to have sizable quasifission contribution in addition to the compound nuclear fission component in the fusion–fission reaction. The mass distribution of the fission fragments is another quantity which can be used to disentangle between compound nuclear and non-compound nuclear fission. This

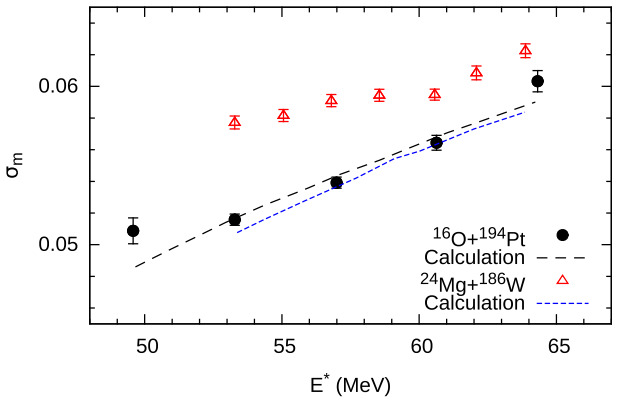

Figure 11. Experimental mass ratio width (σ_m) values for the two reactions compared with the calculations based on compound nuclear process as discussed in ref. [30].

has been exploited by a number of groups [30,73–80]. We shall give one example from the work of Prasad *et al* [30]. They measured the fission fragment mass ratio distributions and mass–angle correlations for the two systems $^{16}O + {}^{194}Pt$ and $^{24}Mg + {}^{186}W$ forming the same compound, ^{210}Rn (figure 11). Mass–angle correlation has been taken as evidence for the presence of quasifission in the measured reaction. However, while neither of the above systems exhibited the mass–angle correlations expected for quasifission, the Mg system showed values of mass ratio distribution width significantly different and larger when compared to pure compound nucleus estimates implying the onset of quasifission in the reaction involving ^{24}Mg and ^{186}W. It may be mentioned that the $Z_P Z_T$ value for this system is only 908 which is significantly less than the value of 1600, usually taken as the threshold value for the onset of quasifission. Further, while the systems $^{24}Mg + {}^{186}W$, $^{30}Si + {}^{186}W$ and $^{34}S + {}^{186}W$ have clearly exhibited non-compound nucleus fission features consistent with the quasifission, their fissility values are less than 0.723, the threshold value for the onset of quasifission. A number of researchers [30,73–80] have carried out measurements of fission fragment mass ratio and their widths for a variety of systems and have come out with varying conclusions about the presence of quasifission. More recently, the Canberra group has come out with a systematics of mass–angle distributions [79]. Nishio *et al* [80] have indicated that the non-compound nucleus fission events can get mixed with the mass symmetric fission fragments, usually taken to be of pure compound nucleus origin. It is very important to take this fact into account in the analysis to extract information about compound nucleus fission from the measured mass distribution data. The above examples demonstrate the importance of dynamics in the nuclear fission process.

4.2 *Nuclear structure at the saddle point*

The most fundamental quantity in nuclear fission is the fission barrier. An approximate value of the barrier was derived by Bohr and Wheeler way back in 1939 using the charged liquid drop model. As we mentioned, the single-particle aspects were introduced in

addition to the macroscopic features to describe the fission phenomena. As a result, the estimated liquid drop barrier got revised in a number of cases. Extensive measurements and analysis of fission excitation functions have been carried out in the last 75 years to determine the fission barrier heights. Initially, the measurements were carried out using n, p, α and γ-rays. Later on, with the advent of heavy-ion accelerator, focus has shifted towards heavy-ion induced fission. In the actinide region, the fission barrier heights are of the order of 6 MeV. In this region, fission barrier can be measured from the measured neutron-induced fission excitation functions, which exhibit the characteristic rise followed by a flat plateau. However, the fission barrier heights for the pre-actinide nuclei are not known with similar accuracy. For these nuclei, the fission barrier heights are significantly large when compared to the neutron separation energy. As the fission cross-sections are extremely small, they are generally not available at low neutron energies. Generally, the barriers are extracted from a statistical model analysis and hence the determinations of fission barrier will have the uncertainties associated with the model and the other parameters used in the analysis. The study of the fission fragment angular distributions yields information regarding the saddle point, one of the decision-making points in the fission decay of the nucleus. The other critical point in the decay process is the scission point.

From a series of fission fragment angular distribution measurements followed by analysis using the saddle-point statistical model, the success of this model in describing a large body of fission data has been demonstrated [2]. The statistical decay of the excited compound nucleus is usually depicted as follows: Basically it is a competition between the neutron and the fission decay (see figure 8). The expression for the fission and neutron emission decay widths are given in eqs (1)–(3). The fission barrier and the level density parameters are the main ones to be optimized to fit a given data as B_n is estimated by knowing the masses. In performing the statistical model analysis, we require a number of input parameters – masses of the projectile, target, intermediate compound nucleus and the other nuclei produced after neutron evaporation, the level densities at the equilibrium deformation, at the saddle point and the equilibrium deformation of the residual nucleus after neutron evaporation, the fission barrier, the neutron optical model etc. D'Arrigo *et al* [81] have proposed a statistical model analysis of the fission data to estimate the temperature- and angular momentum-dependent shell corrections. For the present discussion we shall limit to only three quantities which are the most sensitive, viz. the fission barrier, the shell corrections and the level density parameters.

4.2.1 *Fission barrier and shell correction at the saddle point*

It is known that if we had only evaporation residue and fission cross-sections, it is not possible to obtain unique values of barrier and level density parameters from a statistical model analysis of the data. However, if we add the pre-fission neutron multiplicity data, then it is possible to constrain the parameters rather uniquely from a statistical model analysis. This fact has been brought out recently by Mahata *et al* [82].

A schematic representation of potential energy as a function of deformation is shown in figure 12. The deformation energy has contribution from the smoothly varying liquid drop part and from the oscillatory shell correction. As shown in figure 12, fission barrier can be expressed as, $B_f = B_{LD} - \Delta_n + \Delta_f$, where B_{LD}, Δ_n and Δ_f are the liquid drop fission barrier, the ground-state shell corrections and the shell correction at the saddle point,

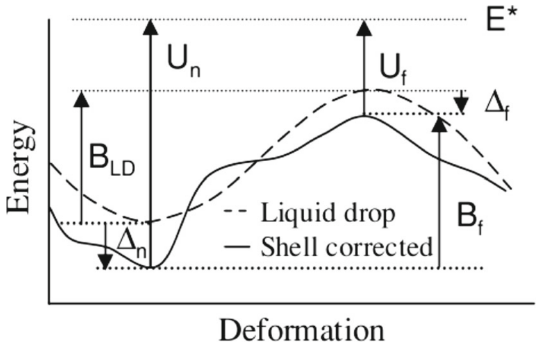

Figure 12. Fission barriers and the shell corrections at the ground state and the saddle point. B_{LD} is the liquid drop barrier. The Us are the excitation energies above the ground state and the saddle point (ref. [82]).

respectively. The available thermal excitation energy (U) at the equilibrium deformation as well as at the saddle point depends on the shell corrections at the respective places. The shell correction at the equilibrium deformation (the ground state) is obtained as $\Delta_{\mathrm{n}} = M - M_{\mathrm{LD}}$, the difference between the experimental and the liquid drop masses. Experimental information about the shell correction at the saddle point for nuclei with mass $A \sim 200$ is scarce. Mahata *et al* have expressed saddle-point shell correction as, $\Delta_{\mathrm{f}} = k_{\mathrm{f}} \times \Delta_{\mathrm{n}}$, where k_{f} is obtained by a fit to the data. An energy-dependent shell correction of the level density parameter is taken as

$$a_x = \tilde{a}_x[1 + (\Delta_x/U_x)(1 - \exp(-\eta U_x))], \tag{12}$$

where $x = \mathrm{n}$ or f.

Although the collective enhancement in level density and the reduction of fission width (Kramers factor) due to dissipation have not been considered explicitly in the analysis, it has been found that the fission barrier or the shell correction at the saddle point is not very sensitive to these factors. The ratio of the asymptotic value of the level density parameter at the saddle deformation to that at the equilibrium deformation ($\tilde{a}_{\mathrm{f}}/\tilde{a}_{\mathrm{n}}$) is found to be sensitive to the collective enhancement and Kramers factor. A consistent analysis using the statistical model has yielded nearly 50% of the ground-state shell correction at the saddle point. In the analysis, Mahata *et al* have corrected the measured ν_{pre} for dynamical emission corresponding to a dynamical delay of 30×10^{-21} s. However, if the actual dynamical delay is larger or there are other non-statistical contributions (e.g. near-scission emission), the required value of the shell correction at the saddle point will reduce. A typical result is shown in figure 13 [82]. The calculations are also sensitive to the collective enhancement in the level densities expected at the saddle due to larger deformation when compared to the ground state [84]. The presence of significant shell correction at the saddle point estimated using the prescription of ref. [82], is an important finding. From a detailed statistical model analysis of a number of nuclei, covering a range of isotopes, it has been found that the deduced fission barrier (liquid drop part) decreases with decrease in neutron number of a given Z of the nucleus [85]. Further, these values are significantly lower than the theoretical estimates [86,87] implying the possible role

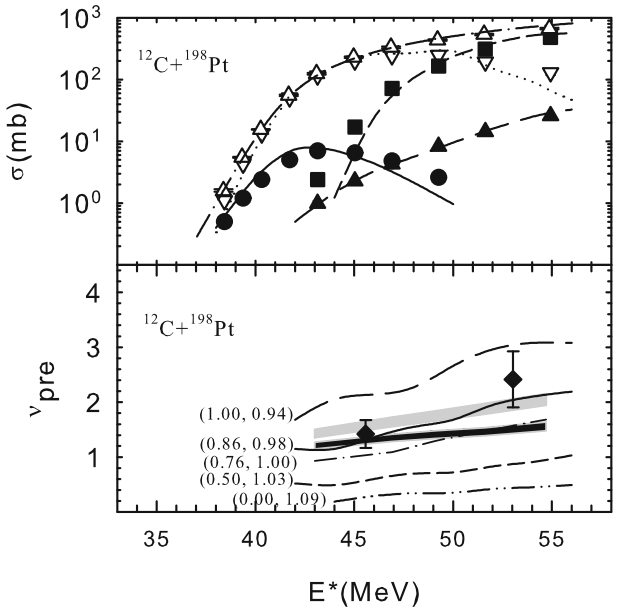

Figure 13. The experimental data for cross-section (open triangle – fusion, filled triangle – fission, filled circle – 3n channel, inverted triangle – 4n channel, filled square – 5n channel) and pre-fission neutron multiplicity (ν_{pre}) are compared with the statistical model calculations. The values in brackets represent k_f and $\tilde{a}_f/\tilde{a}_n$. The grey band represents the multiplicity values as obtained from the systematics [83]. The above multiplicity values corrected for the dynamical emission corresponding to a dynamical delay of 30×10^{-21} s (see ref. [82]) are represented by the black band.

of nuclear structure. Nath *et al* [88], from an analysis of the fusion data for a number of nuclei (compound nuclei having $Z = 80, 82, 83$ and 85), have observed an interesting correlation of B_f with the magicity, $Z = 82$. They found that while the B_f values for $Z = 80$ and 82 are nearly the same, there is a noticeable drop in the B_f value for $Z = 83$. They also found that the deduced barriers were somewhat smaller than the estimates of ref. [87]. A number of investigators have used the relation $B_f = C \times B_{LD} - \Delta_n$ and obtained a value of 0.6 to 0.8 for the normalization constant C and no explicit shell correction at the saddle point. If we relate this relation for fission barrier to the earlier one proposed by Mahata *et al* [82], one can obtain the shell correction at the saddle point $-\Delta_f = (1 - C)B_{LD}$. Putting the value of 0.6 to 0.8 for C, we get that the shell correction at the saddle could be varying from 40 to 20% of the B_{LD}. Additional data of the fission fragment angular distributions, the spin distributions and the fission events corresponding to the first, second and third chance fission will be helpful to constrain the statistical model parameters and make a reliable estimate of the shell correction at the saddle.

The fission barrier is given as the sum of the liquid drop barrier and the shell correction at the equilibrium deformation. It is generally assumed that the shell effects are not significant at the saddle. However, there is no fundamental reason to leave out shell effect at the saddle, either in dealing with the level density at the saddle or the shell correction at the saddle in determining the effective fission barrier. The liquid drop values of the

fission barriers are given by several methods: the rotating liquid drop model (RLDM) [89], the rotating finite range model (RFRM) [86] and the Thomas Fermi model (TFM) [87]. According to Myers and Swiatecki [87] the liquid drop fission barrier can be given as

$$B_f(Z, N) = S(Z, N)F(X). \tag{13}$$

Here

$$S = A^{2/3}[1 - kI^2] \tag{14}$$

with $k = 1.9 + [(Z - 80)/75]$ and $I = (N - Z)/A$,

$$F(X) = \begin{cases} 0.000199748(X_0 - X)^3 & \text{for } X_1 \le X \le X_0 \\ 0.595553 - 0.124136(X - X_1) & \text{for } 30 \le X \le X_1 \end{cases} \tag{15}$$

with $X = Z^2/[A(1 - kI^2)]$, $X_0 = 48.5428$ and $X_1 = 34.15$.

We have estimated the effective barriers at the saddle, by adding the ground-state shell correction from Moller *et al* [90] to the liquid drop barrier from the Thomas Fermi model for a few nuclei where shell corrections are significant. If shell correction at the saddle is 100% of the ground-state value, then the two shell correction terms Δ_n and Δ_f cancel. The barrier value becomes equal to the liquid drop value. If there is 0% shell correction, then the barrier value is given as the sum of the liquid drop and ground state shell corrections. IIjinov *et al* [91] have shown that it is possible to obtain a fit to the data with or without shell correction, by suitably adjusting the other parameters. It may be mentioned that the B_f value determined is dependent on the a_f/a_n value assumed. Usually, the ratio of the level density parameters is a few percent greater than one to take into account the fact that the level densities at the saddle will be larger for a given excitation energy due to deformation at the saddle. Mahata *et al* [82] have shown that it is possible to fit the fission and evaporation residue data for various combinations of B_f and a_f/a_n (see figure 13). Whether or not shell correction is significant at the saddle will be brought out more clearly by analysing the data of a series of isotopes of Hg and Po, where it is seen that the ground-state shell corrections vary significantly over the isotopes. From the limited comparison of the estimates and the experimental values (table 1) of the fission barriers (determined from a statistical model analysis), it is not possible to rule out the presence of shell effect at the saddle. All these experimental values of fission barriers have been obtained exclusively by analysing the of cross-section data. As it was discussed earlier, the additional data of neutron multiplicity clearly reveal the need for significant shell correction at the saddle point. In a recent work, Golda *et al* [95] have shown that the fission barrier values could be different from the values given in the table if the fission data are analysed including the pre-fission neutron multiplicity values. Further, the macroscopic fission barriers obtained for some nuclei using the beta-delayed fission approach are found to be smaller when compared to the predictions of refs [86,87].

D'Arrigo *et al* [81] have carried out a comprehensive statistical model analysis of both the light and the heavy ion data. They have parametrized the shell effect in terms of temperature and angular momentum and the gradual fading out of the shell effect at higher excitation energies. They have considered the proton data to fix the temperature dependence of shell effect as the angular momentum effects will be less in these data. By combining the heavy-ion data they have been able to get a handle on the angular momentum dependence of the shell effect. They have concluded that the effective fission barriers

Table 1. Fission barriers for a few nuclei near the magic number $Z = 82$.

Nucleus	A	TF value B_{LD} (MeV)	Δ_{n} (MeV)	$B_{\mathrm{f}} = B_{\mathrm{LD}} - \Delta_{\mathrm{n}}$ (MeV)	Experimental B_{f} (MeV)
Hg, $Z = 80$	196	16.0	−4.5	20.5	16.9[a], (18.7, 20.7)[b]
	198	16.5	−6.0	22.5	16.6[a], (19.5, 21.8)[b]
	200	17.0	−7.5	24.5	17.7[a], (21.2, 24.5)[b]
	202	17.4	−9.1	26.5	
	204	17.8	−10.7	28.5	
	206	18.1	−12.0	30.1	
Po, $Z = 84$	202	10.08	−4.6	14.7	
	204	10.48	−6.3	16.8	14.0[c]
	206	10.88	−8.07	19.0	17.2[c]
	208	11.21	−9.44	20.7	19.9[a], (17.9, 20.2)[b] 19.7[c]
	210	11.53	−10.84	22.4	21.2[a], (18.2, 21.3)[b], 23.9[d], 21.7[c]
	212	11.78	−8.7	20.5	19.6[a], (16.3, 19.7)[b], 22.0[d], (17, 18, 18.5)[e]

[a]Ref. [92]
[b]Ref. [93]
[c]Ref. [84]
[d]Ref. [94]
[e]Ref. [91]

obtained from the statistical model analysis of the heavy-ion data (generally available at higher excitation energies) are likely to be consistent with the macroscopic droplet model predictions. They also expect the barriers determined by the analysis of light-ion data (extending to lower excitation energies) to be in agreement with the values of the model which includes both macroscopic and microscopic aspects. In essence, for the same compound nucleus, the difference in barriers extracted from the analysis of light- and heavy-ion data could differ as much as the ground-state shell correction. There is a need to carry out a careful analysis of the data which should include not only cross-sections but also anisotropies and pre-fission particle multiplicities to determine the fission barrier more reliably. It must be stated that the determination of the barrier (B_{f}) from a statistical model analysis is strongly dependent on the other parameters used in the calculation, in particular the ratio of the level densities, $a_{\mathrm{f}}/a_{\mathrm{n}}$. However, the calculation of the barrier from theory based on potential energy surface is devoid of these limitations. Hence a caution is needed when a comparison is made of the fission barrier estimated from the experiment and the theory.

4.2.2 *Effective moment of inertia at the saddle point of the fissioning nucleus*

The fission angular distributions are sensitive to the deformation at the saddle point in employing the saddle point model. According to this model, the fission anisotropy (A) is

related to $\langle \ell^2 \rangle$, the second moment of the compound nuclear spin distribution (contributing to fission), T, the temperature at the saddle and I_{eff}, the effective moment of inertia at the saddle deformation as given in eq. (8). The moment of inertia (and K_0^2) can be deduced from an analysis of the fission angular distribution by knowing the values of $\langle \ell^2 \rangle$ and T.

The determination of I_{eff} has been pursued almost right from the inception of the discovery of nuclear fission as it is related to the deformation of the fissioning nucleus. Several systematic studies of this quantity have been carried out as a function of the fissility of the fissioning nucleus [2,4,5,39,96–99]. Many years ago, Vaz and Alexander [4] have made a reassessment of the angular distributions of fission fragments from continuum states in the context of transition state theory and analysed a large number of systems populated by light and heavy ions with a range of spin and excitation energies. Mahata *et al* [99] have analysed the fission fragment angular distributions of a number of systems with $A \approx 200$–210. It is generally found that the values of the moment of inertia required to fit the fission angular distribution data are about 10% less when compared to that obtained by Sierk [86] using the rotating finite range model. Vandenbosch [100] has extracted I_{eff} values from the experimental angular distributions for several systems covering a wide range of Z^2/A. Experimental I_{eff} values were compared with the macroscopic liquid drop models of Cohen–Plasil–Swiatecki (CPS) [89] and Sierk [86]. While the experimental results are found to be in good agreement with the prediction of Sierk for large values of Z^2/A, they are found to be more close to CPS for smaller values of Z^2/A. It will be interesting to study the behaviour for intermediate values of Z^2/A. It has been reported recently by Soheyli [98] that the average I_{eff} values obtained (averaged over a range of bombarding energies) are consistent with the RLDM values for the light-ion-induced reactions and in good accord with the RFRM predictions in the case of heavy-ion-induced reactions (similar to the conclusions drawn by Vandenbosch [100]). The RFRM and RLDM values along with the experimental values of I_{eff} obtained for a number of systems are plotted in figure 14 as a function of the mass number of the fissioning compound nucleus. It appears that for the actinides, the RFRM does a better job in reproducing the values of the moment of inertia obtained experimentally.

In ref. [98], the quadrupole deformation and mass asymmetry parameters of the fissioning nuclei at the saddle point are also estimated from the fission data. Again it may be emphasized that to arrive at a reliable estimate of the moment of inertia of the saddle point, it is necessary to separate the pure compound nuclear fission events from the total fission events (see the earlier discussions in §3 and 4). Theoretically, the values of the effective moment of inertia have been calculated using the rotating liquid drop model (RLDM) [89] and rotating finite range model (RFRM) [86]. The extracted I_{eff} will be sensitive to the compound nucleus spin distribution and T. The T is dependent on the chance of fission and the level density parameter. If the saddle point is used, then the moment of inertia will correspond to the saddle-point deformation. If the analysis is carried out using the scission point model, then the moment of inertia will correspond to that deformation. Friefelder *et al* [5] have compared the K_0^2 values with the predictions of the transition state models – the saddle-point and the scission-point models. They have reported that the experimentally determined values lie in general between the saddle- and scission-point predictions. According to Newton [7], this implies that the decision-making point in fission is perhaps in between the saddle and the scission points. Perhaps, a dynamic model where the

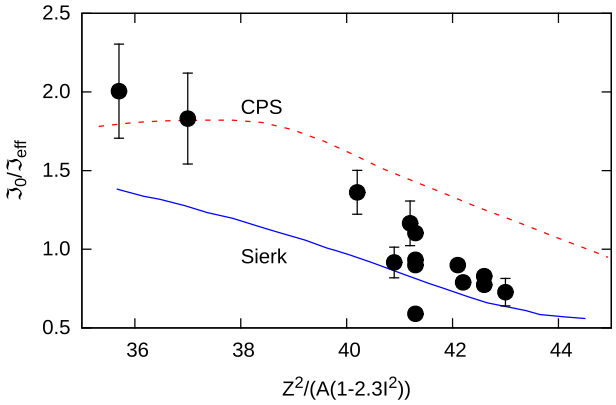

Figure 14. A plot of the effective moment of inertia I_{eff} at the saddle (scaled by the moment of inertia I_0 of the spherical compound nucleus) against the fissility parameter, $Z^2/(A(1-2.3I^2))$. $I = (N-Z)/A$. The experimentally deduced values are taken from ref. [100]. The dashed line and the continuous line represent the RLDM (CPS) and RFRM (Sierk) predictions.

fissioning nucleus is described from the equilibrium deformation to the scission point will be able to provide a clear answer for this. For fissioning nuclei with axial symmetric ellipsoidal shapes, the moment of inertia parallel and perpendicular to the symmetry axis can be expressed as $I_{\text{pa}} = 0.4AmR^2(1-0.63\beta)$ and $I_{\text{pe}} = 0.4AmR^2(1+0.32\beta)$, where A is the mass number, m is the nucleon mass, R is the spherical equivalent radius of the nucleus and β is the quadrupole deformation parameter. The effective moment of inertia is then written as $I_{\text{eff}} = I_{\text{pe}}I_{\text{pa}}/(I_{\text{pe}} - I_{\text{pa}}) = 0.4AmR^2(1.05 - 0.33\beta)/\beta$. Soheyli [98] has obtained the β values for the three systems $^{11}\text{B} + ^{237}\text{Np}$, $^{12}\text{C} + ^{236}\text{U}$ and $^{16}\text{O} + ^{232}\text{Th}$ systems, all forming the same compound nucleus ^{248}Cf. The β values are respectively for 0.50, 0.55 and 0.52. These values are roughly two times the ground-state deformation value for the nucleus ^{248}Cf. This is consistent with the expectation that the saddle-point deformation will be typically two times the ground-state values. It will be interesting to compare the moment of inertia and deformation values obtained from the analysis of superdeformed nuclei with the ones deduced from the analysis of the fission data. For a comprehensive listing of the statistical model parameters, one can refer to ref. [101] where the reference input parameter library (RIPL) required for performing statistical model calculations is contained.

4.3 *Dissipation – Nuclear viscosity from fission*

We have seen the role of dynamics and structure in influencing the nuclear fission phenomenon. Another important aspect of fission, viz. dissipation, was brought out very early in a pioneering paper by Kramers [34]. He argued that due to the dissipation, a part of the flux at the saddle point of deformation can rediffuse back to the side of equilibrium deformation. This will lead to reduction of the fission decay probability. It was noticed that the dissipative dynamics is also important to understand the most probable kinetic energy carried by the fission fragments [102,103]. In fact, the dissipation in fission has

implication for almost all the fission observables discussed earlier [104]. For the progress made in this field of research, one can refer to some of the following papers [105–109]. In ref. [108], Blocki and Wilczynski have addressed the issue of dissipation in the case of mass drift observed in strongly damped heavy-ion collisions. The experimental observation of pre-fission neutrons significantly larger than the statistical model [7,9,10,37] prediction revived the interest of dissipation in fission phenomenon once again. The energy associated with collective motion is converted to intrinsic excitation energy of the system due to dissipation.

There are a number of observables which have been shown to be sensitive to nuclear viscosity (and related to fission process) – the widths of the giant dipole resonances, in particular of the fissionable nuclei, the kinetic energy and mass distribution in fission, the fission probability and evaporation residue cross-section, the pre-fission particles. Basically, the dissipation effects arise due to two factors: the two-body collisions between the nucleons and the one-body collision of the nucleons with the surface of the nucleus. Further, the probability of two-body collisions also increases near the surface due to the reduced applicability of Pauli principle in the surface region. All these aspects have to be taken into account to understand dissipation. The dissipation strength is also dependent on the excitation energy and the deformation of the fissioning nucleus. In the case of one-body dissipation, the nucleus is treated as if it is a 'gas' with nucleons having long mean free path and colliding with the wall of the nucleus – mean field picture. In this scenario, there are two possibilities. One is the wall (the nucleons collide with the moving wall of the fissioning nucleus) and the other is the window (transfer of nucleons take place from one side to the other side in a dumbbell-shape fissioning nucleus). The collisions take place essentially in the neck region. The wall-plus-window dissipation model [102,103] has been successfully applied to describe the average kinetic energy released in fission. The analysis indicated that the dynamical motion is somewhat overdamped. The parameter related to dissipation (friction/viscosity) is given as $k_s \approx 0.3$ deduced from an analysis of the GDR width and probable kinetic energy of fragments. The two-body dissipation is based on the collisions between the nucleons of the fissioning nucleus. In this picture we bring in 'liquid' like behaviour of the deforming nucleus. The one-body and the two-body dissipation phenomena are expected to have different dependence on T. Hence, by determining dissipation as a function of the excitation energy, it may be possible to get a handle on the mode of dissipation.

The characteristic time associated with the relaxation of the collective motion involved in fission, from the equilibrium shape to the saddle point, is of the order of a few times 10^{-21} s. This is generally very small compared to particle emission time from the compound nucleus. In view of this the dynamical time associated with the collective motion involved in fission was not considered in a statistical model analysis. This picture changed when experimentally a significantly large number of neutrons (the pre-fission neutrons much more than what the statistical model predicted) were measured in several heavy-ion reactions. This could be finally understood by invoking the nuclear viscosity or dissipation effects. In figure 15, we have plotted the calculated neutron lifetime (τ_n) for $^{12}C+^{198}Pt$ system as a function of the excitation energy of the compound nucleus. Further, we estimated the transient time, τ_f – the time taken for the system to relax from the equilibrium ground state to the saddle state, using the expression [9] $\tau_f = (\gamma/\omega)\ln(10B_f/T)$, where T is the saddle-point temperature (taken to be 1.5 MeV), γ is the friction coefficient

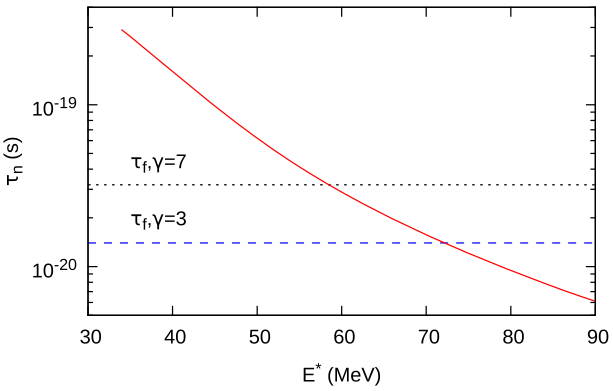

Figure 15. Plot of the neutron lifetime vs. the excitation energy of the compound nucleus.

and ω is the barrier assault frequency (assuming $\omega = 10^{21}$/s). For the present case with the values given above, the τ_f value is 1.4×10^{-20} s for $\gamma = 3$ and 3.2×10^{-20} s for $\gamma = 7$ respectively. It can be seen from figure 15, that for excitation energies below 50 MeV, the neutron lifetime (τ_n) is significantly larger when compared to τ_f. However, for excitation energies from 60 MeV or so, the neutron lifetime becomes comparable to τ_f. In essence, the time taken for the fission degree of freedom – time to deform from the equilibrium shape to the saddle shape – is no longer small compared to neutron emission time. Fission is further slowed down due to the fact that part of the flux above the saddle can diffuse back to the equilibrium shape region due to dissipation, a fact pointed out by Kramers long time ago. The frictional forces (viscosity) affect the time taken to go from the equilibrium to the saddle and also the probability of transmission through the saddle. Using the neutron lifetime varying with excitation energy as a clock, one can measure the transient time (fission delay) in fission for the first time. During the time the fission degree evolves and reaches a steady state, additional neutrons can be emitted. The number of neutrons emitted will strongly depend on the transient time. By invoking the argument of delay in fission due to transient time, it has been possible to account for the extra neutrons measured as pre-fission neutrons.

In general, the total time for the fission to take place in a collision involving a projectile and a target and through a compound nucleus, is $\tau = \tau_f + \tau_{ss} + \tau_{fo}$, where τ_{ss} is the time taken to go from the saddle to the scission (again influenced by viscosity of the nuclear fluid) and τ_{fo} is the formation time of the compound nucleus (capture of the projectile by the target to form the composite system followed by the evolution of this intermediate system towards the fully equilibrated compound nucleus). It has been shown by Saxena *et al* [37] that the last component of time could depend on the entrance channel of the interacting projectile and the target. From a series of experiments the transient and saddle–scission times have been determined and they are of the order of 10^{-20} s. As the fissioning system evolves from the saddle configuration to the scission shape, there is a reduction in the potential energy (30 to 40 MeV). It is of interest to know how this energy is transferred to intrinsic excitation energy and kinetic energy carried by fragments. This will be strongly dependent on the viscosity of the nuclear fluid, in particular

in the saddle to scission region. Adeev *et al* [106] have shown that in the case of models using only two-body dissipation, the values of the viscosity varies from about 3×10^{-23} MeV s/ fm^3 (0.05 TP) (to explain the kinetic energy distribution) to 15×10^{-23} MeV s/ fm^3 (0.15 TP) (to explain the pre-fission neutron data). However, in the case of models using only one-body dissipation, the k_s parameter (related to dissipation) varies from 0.25 to 0.5 to explain the kinetic energy and pre-fission particle data. It may be noted that this is also consistent with the value 0.27 deduced for this parameter from an analysis of GDR widths. There are other reports which indicate that the viscosity values are around 1–2 $\times$ 10^{-23} MeV s / fm^3 [110]. Naderi [109] has extended the multidimensional Langevin equation to four dimension by including the K degree of freedom (projection of spin on the symmetry axis).

It appears that the fission time determined varies from about 5 to 100 $\times$ 10^{-21} s to describe the various observables. In the literature, various symbols have been used for dissipation/friction/viscosity and one has to be careful in comparing different predictions. Aritomo and Chiba [43] have shown that dissipation effects have to be included in their dynamical model calculations, though their effects on the widths of mass distribution are not pronounced. In general, the threshold excitation energy for the appearance of dissipation is around 50 MeV, Saxena *et al* [111] and Strecker *et al* [111] have observed the dissipation effect even at somewhat lower excitation energies. Thoennessen and Bertsch [112] have provided systematics of the threshold for dissipation in fission. There have been some reports that the threshold excitation energy where the fission delay effect has been seen through the neutron lifetime measurements (see figure 15) varies with the neutron shell closure $N = 126$ of the compound nucleus [113]. In order to investigate further the correlation between the threshold excitation energy for the observation of fission delay with the shell closure of the compound nucleus, Singh *et al* [114] have carried out a systematic measurement of the fission and the evaporation cross-sections along with the neutron multiplicities for the three systems, $^{19}\mathrm{F} + {}^{194,196,198}\mathrm{Pt}$ populating compound nuclei with $N = 126$, 128 and 130, over a range of excitation energies. They found that the data for the system with $N = 126$ require lesser dissipation strength when compared to that needed to describe the data for the other two systems. More work of this type will be required to understand the connection between the dissipation and shell closure as we have stated earlier that dynamics, structure and dissipation are all needed to describe the features of fission. The dissipation mechanism certainly plays a crucial role in the transfer of collective energy to kinetic energy of the fissioning nucleus. It is clear that a consistent description taking into account all aspects – dynamics, structure and dissipation – is essential to describe the fission data.

5. Prospects for nuclear fission research

The fission phenomenon continues to be exciting and challenging even after 75 years of its discovery. It is very important to disentangle between different reaction mechanisms and obtain the pure compound nuclear contributions before an attempt can be made to interpret the data. The measurement of fission angular distributions and mass ratio distributions offers an excellent avenue for determining the compound and non-compound fission mechanisms. The nuclear structure at the deformed saddle is interesting, and

systematic data to establish the shell effect at the saddle point more conclusively are required. A rich interplay and delicate balance between the microscopic (shell closure) and the macroscopic (potential energy landscape) has been brought by the mass distribution measurements for proton-rich and neutron-rich Hg isotopes. The current interest and the emerging directions in this field of research are adequately covered in refs [16–18]. Some of the areas of current active interest which hold promise for future research are:

(1) Measurement of mass distributions with improved mass/charge resolution and understanding the behaviour of mass distribution, in particular the near constancy of the charge number of heavy fragment and the evolution of asymmetric to symmetric fission. Recent experimental techniques for the measurement of data of this type are discussed in refs [14,16–18,26–28].
(2) Measurement of pre-fission neutrons and separation of different sources of neutron emission as a function of dynamical evolution of the fissioning nucleus from the equilibrium shape to scission point through the saddle point.
(3) Investigation of the fission of neutron rich/poor nuclei and the evolution of the structure and the dynamics. This aspect is important in the quest for superheavy nuclei.
(4) Role of isospin in fission needs to be substantiated. In this context, mention may be made of the recent work on fission fragment spectroscopy using heavy ions on actinide targets [115].
(5) The interest in the determination of shell effect at the saddle point was catalysed by the work of Shrivastava *et al* [116]. They reported anomalous fission anisotropies for closed shell compound nucleus with $N = 126$. Later, Mahata *et al* [82] carried out extensive work, including fission, evaporation residue cross-sections and pre-fission neutron data to obtain shell effect at the saddle point. It is reiterated that reliable determination of shell effect at the saddle can be achieved by measuring as many observables as possible and over a range of isotopes, followed by a comprehensive analysis in a consistent manner. Both light and heavy ion data, spanning a range of excitation energies, should be considered to take into account the effects due to angular momentum and temperature. In this context it may be remarked that if shell effects at the saddle for the lighter pre-actinides with $N = 126$, are indeed significant then the question is whether these nuclei will exhibit double humped fission barriers [3].
(6) Theoretical efforts to combine both the statistical and dynamical aspects of fission to predict the various quantities measured must be vigorously pursued by comparing more data with the theoretical predictions. In particular, a full understanding of the various aspects of mass distribution data through the macroscopic and microscopic aspects of fission needs further work. It is clear that the statistical, dynamical and dissipative aspects have to be incorporated in any theory used to describe the fission phenomena.
(7) Measurement of fission cross-section for actinides, in particular the ones with short halflives, either through direct or surrogate method [117–119] will be not only of fundamental interest but also very important for nuclear reactor programmes in general. BARC group [118,119] has been spearheading these efforts in view of our interest in obtaining nuclear data for the Th–U fuel cycle.

(8) The shell effect at large deformation has been the driving factor for our expectation for the existence of superheavy nuclei. Considerable efforts are underway to populate the superheavy nuclei using combinations of targets and projectiles. Currently, the search is on for the superheavy nucleus with $Z = 120$. While these painstaking efforts will continue, there are also investigations aimed at the study of fission decay of moderately excited superheavy nuclei formed in heavy-ion reactions. The BARC–INFN Collaboration has made careful measurements in this direction. The results for ^{80}Se + ^{208}Pb and ^{232}Th which populate $Z = 116$ and 124 have been reported [120]. For example, the total neutron multiplicity deduced for the spontaneous fission of $Z = 124$ nucleus is around 15, a value consistent with the large values expected for the superheavy nuclei. This is also another interesting area where more experimental investigations are fruitful. It may be pointed out that so far no evaporation residue (ER) cross-section has been reported for such a target–projectile system. It will be useful to carry out neutron multiplicity measurements for composite systems where the corresponding ER cross-sections have been reported, to establish the correlation between the neutron multiplicity with the mass/charge of the composite system.

(9) As pointed out, the structure, the dynamics and the dissipation are essential to describe the fission observables. More systematic work to get further insights into dissipation or viscosity mechanism in fission is desirable.

6. Conclusion

Some of the highlights of nuclear fission studies carried out using light and heavy ions have been covered in this review. The challenges, both in experimental and theoretical investigations, involved in obtaining reliable information about the fissioning nucleus have been elaborated. It has been pointed out that the nuclear fission phenomenon provides ample scope to understand the behaviour of nuclei at large deformation, angular momenta and isospin values. Both single-particle and collective features are exhibited in this process. A dynamical theory is necessary to understand the fission process and the various observables. New data particularly from both neutron-rich and neutron-deficient regions will be helpful to compare the data with the existing knowledge for nuclei away from the line of stability. With increasing availability of intense ion beams, both stable and radioactive, coupled with more efficient detector arrays, nuclear fission research is poised for exciting times in terms of new findings and improved understanding of this phenomenon.

Acknowledgement

The authors were greatly inspired by discussions on nuclear fission with late Dr M K Mehta, Prof. R Vandenbosch, Dr S S Kapoor and Dr V S Ramamurthy. The authors thank collaborators from India and abroad for their inputs. The authors thank Dr A Shrivastava for a careful reading of the manuscript and useful suggestions. SK would like to thank Prof. Rohini Godbole, Chief Editor, *Pramana – J. Phys.* for the kind invitation to write this review article. The authors also acknowledge the useful suggestions received from the anonymous referees. SK would like to acknowledge DAE for the support through the Raja Ramanna fellowship.

References

[1] N Bohr and J A Wheeler, *Phys. Rev*. **56**, 426 (1939)
[2] R Vandenbosch and J R Huizenga, *Nuclear fission* (Academic Press, New York, 1973)
[3] S Bjornholm and J E Lynn, *Rev. Mod. Phys.* **52**, 725 (1980)
[4] L C Vaz and J M Alexander, *Phys. Rep.* **97**, 1 (1983)
[5] R Freifelder, M Prakash and J M Alexander, *Phys. Rep.* **133**, 315 (1986)
[6] S S Kapoor, *Workshop on Applied Nuclear Theory and Nuclear Model Calculations for Nuclear Energy Applications* edited by M K Mehta and J J Schmidt (World Scientific, 1988) p. 537
[7] J O Newton, *Sov. J. Nucl. Phys.* **21**, 349 (1990); *Pramana – J. Phys.* **39**, 175 (1989)
[8] C Wagemans, *The Nuclear fission process* (CRC Press, Boca, Raton, 1991); The two special issues brought out on the occasion of 50 years of nuclear fission, *Nucl. Phys. A* **502**, 1-630c (1989); *Pramana – J. Phys.* **33**, 1 (1989)
[9] R Vandenbosch, *RIKEN winter school on new facets of nuclear reactions* (Yuzawa, Japan, 1993)
[10] D Hilscher, I I Gontchar and H Rossner, *Phys. At. Nuclei* **57**, 1187 (1994)
D Hilscher and H Rossner, *Ann. Phys. Fr.* **17**, 471 (1992)
[11] S Kailas, *Phys. Rep.* **284**, 381 (1997)
[12] R K Choudhury and S S Kapoor, *Proc. Indian National Science Academy* **66**, 599 (2000)
[13] S Kailas *et al*, *Nucl. Phys. A* **787**, 259c (2007)
[14] K H Schmidt and B Jurado, *EPJ Web of Conferences* **62**, 06001 (2013)
K H Schmidt, *Joliot Curie School "Physics on the femtometer scale"* (2011) (unpublished)
[15] *EPJ Web of Conferences* **17** (2011); *J. Phys: Conf. Ser.* **282** (2011)
[16] *5th Advanced Science Researh Center International Workshop on Perspectives in Nuclear Fission* (JAEA, Tokai, 2012)
[17] *10th Advanced Science Research Center (ASRC) International Workshop on Nuclear Fission and Decay of Exotic Nuclei* (JAEA, Tokai, 2013)
[18] *Institute for Nuclear Theory Workshop – Quantitative Large Amplitude Shape Dynamics: Fission and Heavy Ion Fusion* (Seattle, 2013)
[19] A N Andreyev, M Huyse and P Van Duppen, *Rev. Mod. Phys.* **85**, 1541 (2013)
[20] O Hahn and F Strassmann, *Naturwiss*. **27**, 11 (1939); *ibid.* **27**, 89 (1939)
[21] K Mahata *et al*, *Nucl. Phys. A* **720**, 209 (2003)
[22] S Kailas *et al*, *Phys. Rev. C* **59**, 2580 (1999)
[23] M B Chadwick *et al*, *Nucl. Data Sheets* **112**, 2887 (2011)
[24] P Armbruster *et al*, *Nucl. Instrum. Methods* **139**, 213 (1976)
G Fioni *et al*, *Nucl. Instrum. Mehtods A* **332**, 175 (1993)
[25] K H Schmidt *et al*, *Nucl. Phys. A* **665**, 221 (2000)
[26] F Farget *et al*, *J. Phys: Conf. Ser.* **420**, 012119 (2013)
M Caamano *et al*, *Phys. Rev. C* **88**, 024605 (2013)
[27] K H Schmidt, in refs [14,16,18]
[28] A N Andreyev, in ref [16]
[29] K R Flynn *et al*, *Phys Rev. C* **5**, 1725 (1972)
[30] E Prasad *et al*, *Phys. Rev C* **81**, 054608 (2010)
[31] V Metag, D Habs and H J Specht, *Phys. Rep.* **65**, 3 (1980)
[32] M G Mayer, *Phys. Rev.* **74**, 235 (1948)
[33] V M Strutinsky, *Nucl. Phys. A* **95**, 420 (1967); *Nucl. Phys. A* **122**, 1 (1968)
[34] H A Kramers, *Physica* **7**, 284 (1940)
[35] R G Stokstad, *Treatise on heavy ion science* edited by D Bromley (Plenum, New York, 1985) Vol. 3, p. 83

[36] N D Dang, *Proceedings of ISPUN 11* (Hanoi, 2011)
[37] A Saxena *et al*, *Phys. Rev. C* **49**, 932 (1994)
[38] V E Viola *et al*, *Phys. Rev. C* **31**, 1550 (1985)
[39] B D Wilkins *et al*, *Phys. Rev. C* **14**, 1832 (1976)
[40] U Brosa, *Phys. Rep.* **197**, 167 (1990)
[41] M Warda *et al*, *Phys. Rev. C* **86**, 024601 (2012)
[42] T Ichikawa *et al*, *Phys. Rev. C* **86**, 024610 (2012)
[43] Y Aritomo and S Chiba, *Phys. Rev. C* **88**, 044614 (2013)
[44] J Randrup and P Moller, *Phys. Rev. Lett.* **106**, 132503 (2011); *Phys. Rev. C* **88**, 064006 (2013)
See also some of the early works in this broad area of exchange of nucleons as a stochastic process: R Ramanna, *Phys. Lett.* **10**, 321 (1964)
V S Ramamurthy and R Ramanna, *Proc. of 2nd IAEA Symposium on Physics and Chemistry of Fission* STI/PUB/234, p. 41 (1969) (IAEA-SM-122/15), IAEA, Vienna
[45] A N Andreyev *et al*, *Phys. Rev. Lett.* **105**, 252502 (2010)
[46] A V Andreev *et al*, *Phys. Rev. C* **86**, 044315 (2012); *Phys. Rev. C* **88**, 047604 (2013)
[47] B Back *et al*, *Rev. Mod. Phys.* **86**, 317 (2014)
[48] B Back *et al*, *Phys. Rev. C* **32**, 195 (1985); *Phys. Rev. C* **33**, 385 (1986)
[49] C Ngo, *Prog. Part. Nucl. Phys.* **16**, 139 (1986)
[50] C Lebrun *et al*, *Nucl. Phys. A* **321**, 207 (1979)
[51] B Borderie *et al*, *Z. Phys. A* **299**, 263 (1981)
[52] S Bjornholm and W J Swiatecki, *Nucl. Phys. A* **391**, 471 (1982)
[53] W Shen *et al*, *Phys. Rev. C* **36**, 115 (1987)
[54] J Toke *et al*, *Nucl. Phys. A* **440**, 322 (1985)
[55] V S Ramamurthy and S S Kapoor, *Phys. Rev. Lett.* **54**, 178 (1985)
[56] V S Ramamurthy *et al*, *Phys. Rev. Lett.* **65**, 25 (1990)
[57] B R Behera *et al*, *Phys. Rev. C* **69**, 064603 (2004)
[58] B P Ajithkumar *et al*, *Phys. Rev. C* **77**, 021601(R) (2008)
[59] R G Thomas *et al*, *Phys. Rev. C* **67**, 41601(R) (2003)
[60] R Tripathi *et al*, *Phys. Rev. C* **79**, 064607 (2009)
[61] S Appannababu *et al*, *Phys. Rev. C* **80**, 024603 (2009)
[62] D J Hinde *et al*, *Phys. Rev. Lett.* **89**, 282701 (2008)
[63] R N Sagaidak *et al*, *Phys. Rev. C* **68**, 014603 (2003)
[64] R Tripathi *et al*, *Phys. Rev. C* **71**, 044616 (2005)
[65] K Nishio *et al*, *Phys. Rev. Lett.* **93**, 162701 (2004)
[66] S Mitsuoke *et al*, *Prog. Theor. Phys. Suppl.* **154**, 53 (2003)
[67] J F Liang *et al*, *Prog. Theor. Phys. Suppl.* **154**, 107 (2003)
[68] K Satou *et al*, *Phys. Rev. C* **73**, 034609 (2006)
[69] P Moller and A J Sierk, *Nature* **422**, 485 (2003)
[70] R K Choudhury and R G Thomas, *J. Phys.: Conf. Ser.* **282**, 012004 (2011)
[71] S Soheyli and M K Khalili, *Phys. Rev. C* **85**, 034610 (2012)
[72] H Q Zhang *et al*, *J. Phys: Conf. Ser.* **282**, 012013 (2011)
[73] L M Pant *et al*, *Eur. Phys. J. A* **11**, 47 (2001)
[74] A Yu Chizhov *et al*, *Phys. Rev. C* **67**, 011603 (2003)
[75] R G Thomas *et al*, *Phys. Rev. C* **77**, 0344610 (2008)
[76] R Raefiei *et al*, *Phys. Rev. C* **77**, 024606 (2008)
[77] T K Ghosh *et al*, *Phys. Rev. C* **79**, 054607 (2009)
[78] C Yadav *et al*, *Phys. Rev. C* **86**, 034606 (2012)
[79] R du Rietz *et al*, *Phys. Rev. C* **88**, 054618 (2013)
[80] K Nishio *et al*, *EPJ Web of Conf.* **17**, 09005 (2011)

[81] A D'Arrigo *et al*, *J. Phys. Nucl. Part. Phys.* **20**, 365 (1994)
[82] K Mahata, S Kailas and S S Kapoor, *Phys. Rev. C* **74**, 041301(R) (2006)
[83] H Baba, A Shinohara, T Saito, N Takahashi and A Yokoyama, *J. Phys. Soc. Jpn.* **66**, 998 (1997)
[84] A R Junghans *et al*, *Nucl. Phys. A* **629**, 635 (1998)
[85] R N Sagaidak and A N Andreyev, *Phys. Rev. C* **79**, 054613 (2009)
A N Andreyev *et al*, *Phys. Rev. C* **72**, 014612 (2005)
[86] A J Sierk, *Phys. Rev. C* **33**, 2039 (1986)
[87] W D Myers and W J Swiatecki, *Phys. Rev. C* **60**, 014606 (1999)
[88] S Nath *et al*, *Phys. Rev. C* **81**, 064601 (2010)
[89] S Cohen, F Plasil and W J Swiatecki, *Ann. Phys. (New York)* **82**, 557 (1974)
[90] P Moller *et al*, *At. Data Nucl. Tables* **59**, 185 (1995)
[91] A S Iljinov *et al*, *Nucl. Phys. A* **543**, 517 (1992)
[92] G N Smirenkin INDC (CCP)-359, IAEA, Vienna (1993)
[93] A V Ignatyuk *et al*, *Sov. Part. Nucl.* **16**, 709 (1985)
[94] K Jing, Ph.D. Thesis (U. California 1999) LBNL-43410
[95] K S Golda *et al*, *Nucl. Phys. A* **913**, 157 (2013)
[96] R F Reising, G L Bate and J R Huizenga, *Phys. Rev.* **141**, 1161 (1966)
[97] Y T Oganessian and Y A Lazarev, Heavy ions and nuclear fission, in: *Treatise on heavy ion science* edited by D A Bromley (Plenum Press, New York, 1985) Vol 4, p. 1
[98] S Soheyli, *Phys. Rev. C* **84**, 044609 (2011)
[99] K Mahata *et al*, *DAE Symposium on Nuclear Physics*, **57**, 480 (2012); *ibid* **56**, 490 (2011)
[100] R Vandenbosch, *Proc. Beijing Int. Symp. on Phys. at Tandem* edited by Jiang Chenglie *et al* (World Scientific, 1986) p. 355
[101] *Handbook for calculations of nuclear reaction data*, RIPL-2-IAEA-TECDOC-1506 (2006); RIPL-3, *Nuclear Data Sheet* **110**, 3107 (2009)
[102] W J Swiatecki, *Prog. Part. Nucl. Phys.* **4**, 383 (1980)
[103] J R Nix, *Nucl. Phys. A* **502**, 609 (1989)
[104] P Frobrich and I I Gontchar, *Phys. Rep.* **292**, 131 (1998)
[105] A Di Nitto, *Study of fission dynamics in the composite system of intermediate fissility*, Ph.D. Thesis (U. Napoli, 2009)
[106] G D Adeev *et al*, *Phys. Particles and Nuclei* **36**, 712 (2005)
[107] S Pal and J Sadhukhan, *Pramana – J. Phys.* **82**, 671 (2014)
[108] J Blocki and J Wilczynski, *Acta Phys. Polon. B* **29**, 333 (1998)
[109] D Naderi, *J. Phys. G: Nucl. Phys.* **40**, 125103 (2013)
[110] N Auerbach and S Shlomo, *Phys. Rev. Lett.* **103**, 172501 (2009)
[111] A Saxena *et al*, *Phys. Rev. C* **65**, 064601 (2002)
M Strecker, R Wien, P Pilschde and W Scobel, *Phys. Rev. C* **41**, 2172 (1990)
[112] M Thoennessen and G F Bertsch, *Phys. Rev. Lett.* **71**, 4303 (1993)
[113] B Back *et al*, *Phys. Rev. C* **60**, 044602 (1999)
H Hofmann *et al*, *Phys. Rev. C* **64**, 054316 (2001)
[114] V Singh *et al*, *Phys. Rev. C* **87**, 064601 (2013)
[115] L S Danu *et al*, *Phys. Rev. C* **81**, 014311 (2010)
[116] A Shrivastava *et al*, *Phys. Rev. Lett.* **82**, 699 (1999)
[117] J E Escher *et al*, *Rev. Mod. Phys.* **84**, 353 (2012)
[118] B K Nayak *et al*, *Phys. Rev. C* **78**, 061602 (2008)
[119] V V Desai *et al*, *Phys. Rev. C* **87**, 034604 (2012)
[120] R G Thomas *et al*, *Phys. Rev. C* **75**, 024604 (2007)